2013

RETRACTED ARTICLE: The BCL11A transcription factor directly activates RAG gene expression and V(D)J recombination

Baeck-seung Lee
University of Texas at Austin

Joseph D. Dekker
University of Texas at Austin

Bum-kyu Lee
University of Texas at Austin

Vishwanath R. Iyer
University of Texas at Austin

Barry P. Sleckman
Washington University School of Medicine in St. Louis

See next page for additional authors

AMERICAN SOCIETY FOR MICROBIOLOGY | Molecular and Cellular Biology®

RETRACTION

Retraction for Lee et al., "The BCL11A Transcription Factor Directly Activates RAG Gene Expression and V(D)J Recombination"

Baeck-seung Lee,[a] Joseph D. Dekker,[a] Bum-kyu Lee,[a] Vishwanath R. Iyer,[a] Barry P. Sleckman,[b] Arthur L. Shaffer III,[c] Gregory C. Ippolito,[a] Philip W. Tucker[a]

Institute for Cellular and Molecular Biology, The University of Texas at Austin, Austin, Texas, USA[a]; Department of Pathology and Immunology, Washington University School of Medicine, St. Louis, Missouri, USA[b]; Metabolism Branch, Center for Cancer Research, National Cancer Institute, Bethesda, Maryland, USA[c]

Volume 33, no. 9, p. 1768–1781, 2013, https://doi.org/10.1128/MCB.00987-12. Analysis of our data indicated duplicate bands in Fig. 6E and 7A. It is unclear whether the source of these errors was accidental or purposeful. However, these errors did not change the conclusions of the paper. Nonetheless, we thank the journal for recognizing these errors, and we hereby retract the paper.

Citation Lee B-S, Dekker JD, Lee B-K, Iyer VR, Sleckman BP, Shaffer AL, III, Ippolito GC, Tucker PW. 2017. Retraction for Lee et al., "The BCL11A transcription factor directly activates RAG gene expression and V(D)J recombination." Mol Cell Biol 37:e00358-17. https://doi.org/10.1128/MCB.00358-17.

The BCL11A Transcription Factor Directly Activates RAG Gene Expression and V(D)J Recombination

Baeck-seung Lee, Joseph D. Dekker, Bum-kyu Lee, Vishwanath R. Iyer, Barry P. Sleckman, Arthur L. Shaffer III, Gregory C. Ippolito and Philip W. Tucker

Mol. Cell. Biol. **2013, 33(9):1768. DOI: 10.1128/MCB.00987-12.**
Published Ahead of Print 25 February 2013.

MCB
Journals.ASM.org

The BCL11A Transcription Factor Directly Activates RAG Gene Expression and V(D)J Recombination

Baeck-seung Lee,[a]* Joseph D. Dekker,[a] Bum-kyu Lee,[a] Vishwanath R. Iyer,[a] Barry P. Sleckman,[b] Arthur L. Shaffer III,[c] Gregory C. Ippolito,[a] Philip W. Tucker[a]

Institute for Cellular and Molecular Biology, The University of Texas at Austin, Austin, Texas, USA[a]; Department of Pathology and Immunology, Washington University School of Medicine, St. Louis, Missouri, USA[b]; Metabolism Branch, Center for Cancer Research, National Cancer Institute, Bethesda, Maryland, USA[c]

Recombination-activating gene 1 protein (RAG1) and RAG2 are critical enzymes for initiating variable-diversity-joining (VDJ) segment recombination, an essential process for antigen receptor expression and lymphocyte development. The transcription factor BCL11A is required for B cell development, but its molecular function(s) in B cell fate specification and commitment is unknown. We show here that the major B cell isoform, BCL11A-XL, binds the *RAG1* promoter and *Erag* enhancer to activate RAG1 and *RAG2* transcription in pre-B cells. We employed BCL11A overexpression with recombination substrates in a cultured pre-B cell line as well as Cre recombinase-mediated *Bcl11a*$^{lox/lox}$ deletion in explanted murine pre-B cells to demonstrate direct consequences of BCL11A/RAG modulation on V(D)J recombination. We conclude that BCL11A is a critical component of a transcriptional network that regulates B cell fate by controlling V(D)J recombination.

Recombination-activating gene endonuclease (RAG) catalyzes the cleavage phase of V(D)J recombination (1). RAG is encoded by two adjacent genes, *RAG1* and *RAG2*, whose products must interact to form an active endonuclease (2). Both RAG1 and RAG2 are essential for subsequent B and T lymphocyte development (3, 4). In cell-free systems, RAG1 and RAG2 are sufficient to cleave recombination substrates (1, 5), but *in vivo*, a number of additional factors are required for chromatin accessibility of V(D)J segments and for appropriate completion of the V(D)J joints (6).

RAG expression occurs at two distinct points during B cell development: the first phase results in the assembly of the immunoglobulin heavy chain (IgH) in pro-B cells, whereas the second catalyzes Ig light (L) chain assembly in pre-B cells. RAG expression is tightly regulated at both posttranscriptional and transcriptional levels (6). In addition to the individual promoters for *RAG1* and *RAG2*, the *RAG* locus encodes at least 5 distal enhancer elements: the *RAG* enhancer (*Erag*), the proximal enhancer (*Ep*), the distal enhancer (*Ed*), and two recently discovered regions termed *Irag1* and *Irag2* (7–17) (Fig. 1A). *Erag* is the strongest enhancer, as demonstrated by a 5- to 10-fold reduction in RAG expression and a partial block at the pro-B-to-pre-B transition following targeted deletion of *Erag* in mice (10). A number of transcription factors bind to their corresponding DNA motifs within single or multiple regions within the *RAG* locus (Fig. 1A), and several of these interactions have been shown to activate *RAG* transcription (7, 8, 11, 14, 18, 19).

Originally discovered as the gene disrupted by t(2;14)(p13;q32) translocation in unusually aggressive cases of B cell chronic lymphocytic leukemia (20–23), the B cell lymphoma/leukemia 11A gene (*BCL11A*) was subsequently identified as an Kruppel-like zinc finger oncogene in numerous B cell malignancies (24–29). Among the five BCL11A isoforms previously identified (23, 30), extra long (BCL11A-XL) (NCBI accession number AJ404611) is expressed far more abundantly in hematopoietic lineages (23, 30, 31) (Fig. 1B). All isoforms share a conserved N terminus and an atypical C_2HC zinc finger, which define a "superfamily" of 5 genes essential to myeloid/lymphoid (*EHZF*), megakaryocytic (*FOG1* and *FOG2*), T lymphoid (*BCL11B*), and B lymphoid (*BCL11A*) development (30) (Fig. 1B). Targeted deletion of *Bcl11a* in the mouse indicated that *Bcl11a* is selectively required for progression at the earliest stage (pre-pro-B) of B cell progenitor commitment prior to the RAG-dependent formation of pro-B cells (25). However, a recent study (32) employing a tamoxifen-inducible global *Bcl11a* knockout approach reported the loss of all common lymphoid progenitor (CLP) lineages, including T and NK cells, while sparing myeloid lineages. While resolution of this conflict remains, it is clear from these and other studies (33; G. C. Ippolito et al., submitted for publication) that BCL11A expression commences prior to that of the *RAG* transactivators shown in Fig. 1A, whose expression is lost or highly reduced in *Bcl11a* knockouts (25, 32). Not clear is whether their loss is an indirect result of the strong progenitor block in *Bcl11a*-deficient CLP or whether these factors are direct transcriptional targets of Bcl11a.

Here we identify *RAG1* as a direct target of BCL11A-XL. BCL11A-XL binds within the *RAG1* promoter and *Erag* enhancer to activate *RAG1* and *RAG2* transcription in pre-B cells while repressing *RAG1* promoter activity in epithelial and fibroblast-derived cell lines. Overexpression of BCL11A-XL in a V(D)J recombination-competent pre-B cell line induces *RAG* expression and V(D)J recombination. Cre-mediated deletion of a *lox*-bearing *Bcl11a* locus in cultured pro/pre-B cells abolishes RAG expression and V(D)J recombination. We show that BCL11A-XL either directly or indirectly regulates additional RAG activators as well as

Received 20 July 2012 Returned for modification 25 September 2012
Accepted 14 February 2013
Published ahead of print 25 February 2013
Address correspondence to Philip W. Tucker, philtucker@mail.utexas.edu.
* Present address: Baeck-seung Lee, Department of Pathology and Immunology, Washington University School of Medicine, St. Louis, Missouri, USA.
B.-S.L. and J.D.D. contributed equally to this article.

doi:10.1128/MCB.00987-12

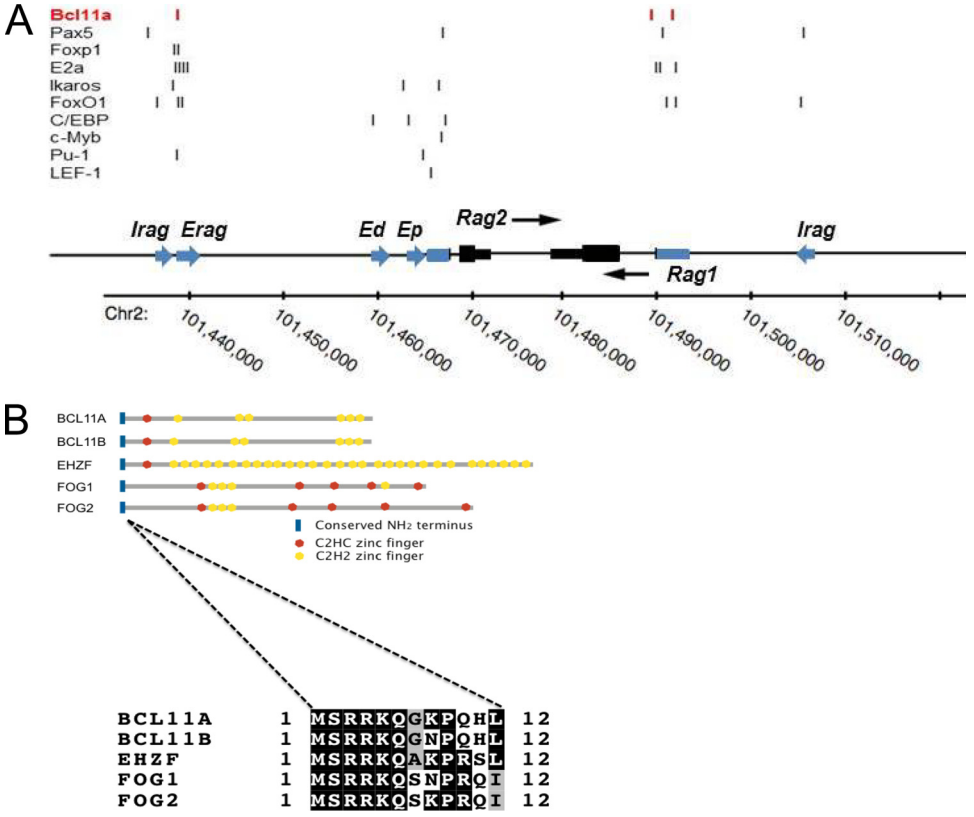

FIG 1 Schematic representation of the *RAG* locus and BCL11A superfamily. (A) Transcriptional regulators and binding regions. The murine *RAG* locus is shown to scale with positions of previously described enhancers (blue arrows), promoters (blue boxes), and exons (black boxes); transcriptional polarity of *Rag1* and *Rag2* is indicated with black arrows. Positions of DNA binding sites for transcription factors determined previously (7, 8, 11, 12, 14, 18, 19, 65) or here (BCL11A-XL) to bind within these regions are indicated by short vertical lines. (B) BCL11A superfamily of transcription factors involved in hematological malignancy. Each member has a highly conserved N terminus, MSRRK (blue), shown in this study to be essential for BCL11A-XL transcriptional activity. This is followed by a single, canonical C_2HC zinc finger (red), which is followed by one or more single, double, or triple zinc fingers of the C_2H_2 type (yellow). BCL11A and BCL11B, as well as early hematopoietic zinc finger (EHZF) and the friend-of-GATA hematopoietic transcription regulators FOG1 and FOG2, encode zinc finger proteins with these conserved features, and several have been implicated in malignancy (23, 26, 30, 45, 58).

activators of *V*κ-*J*κ locus accessibility. We propose that, in addition to its earlier hematopoietic progenitor role, BCL11A is essential for the pro-B-to-pre-B transition, at least in part, from direct loss of V(D)J recombination.

MATERIALS AND METHODS

Mice. C57BL/6 mice with *loxP* sites flanking exons 1 and 2 of *Bcl11a* were generated and genotyped as previously described (29, 34, 35; Ippolito et al., submitted). Mice were bred and housed in the University of Texas animal research facility. All experiments were approved by the IACUC. Four- to six-month-old mice were used for bone marrow (BM) cultures.

Cell culture. Human 293T, human Phoenix, mouse NIH 3T3, and human HeLa cells were maintained in Dulbecco's modified Eagle's medium (DMEM) (Gibco BRL) containing 10% fetal bovine serum (FBS) (HyClone), 100 U/ml penicillin, and 100 μg/ml streptomycin. Human NALM6 pre-B cell and mouse A70 pre-B cell lines were maintained in RPMI 1640 (Gibco BRL) containing 10% FBS (HyClone), 50 μM β-mercaptoethanol, 100 U/ml penicillin, and 100 μg/ml streptomycin.

Pre-B cells were cultured as described previously (36). $B220^+$ cells were isolated from mouse BM using B220-labeled magnetic beads (Miltenyi Biotech). Purified cells were overlaid onto an irradiated S17 stromal cell layer. The cells were maintained in pre-B cell medium (Opti-MEM medium [Gibco] containing 15% FBS, 50 μM β-mercaptoethanol, 2 mM L-glutamine, 100 U/ml penicillin, 100 μg/ml streptomycin, and 5 ng/ml interleukin-7 [IL-7] [R&D Systems]). Cells were passaged every 3 days onto a new S17 stromal cell layer.

Retroviruses and transductions. Human BCL11A-XL cDNA was subcloned into the pXY-IRES-puro (pXY-puro) vector, which was a kind gift from Louis Staudt, National Cancer Institute (37). Mouse stem cell-based retroviruses (MIT [mouse stem cell virus–internal ribosomal entry site–Thy-1.1]) encoding the Cre recombinase (MIT-Cre) and the parental vector (MIT) (8) were gifts of Robert Rickert, Burnham Institute. Mouse stem cell virus encoding the antiapoptotic factor Bcl-x_L (MSCV–Bcl-x_L-Puro) and the stem cell virus encoding the antiapoptotic factor Bcl-x_L were gifts from Robert Rickert, Burnham Institute. Viral DNAs were transfected into the Phoenix-eco cell packaging line by using Fugene (Roche) to produce retroviral particles. Viral particles were harvested 48 h after transfection and centrifuged to remove cell debris. The viral supernatants were ultracentrifuged at 20,000 rpm for 2 h and resuspended in the proper amount of serum-free Opti-MEM medium (Invitrogen).

For pXY-puro viruses, titers were established by infecting NIH 3T3 cells and counting the number of puromycin-resistant cells. Viral particles were incubated with 10 μg/ml of DOTAP liposomal transfection reagent {*N*-[1-(2,3-dioleoyloxy)propyl]-*N*,*N*,*N*-trimethylammonium methylsulfate} (Roche) for 10 min. Various human pre-B and B cell lines were transduced in 24-well culture plates at 25°C by spin inoculation at 1,000 × *g* for 90 min at 30°C. Forty-eight hours after transduction, cells were selected in the presence of 0.5 to 2 μg/ml of puromycin (Sigma).

MIT viruses were preincubated with Polybrene (8 μg/ml) and then diluted 2-fold with Opti-MEM. B220$^+$ BM pre-B cells, following culture (for fewer than 5 passages) as described above, were plated at a density of ~1 × 10^6 cells/ml and 1 day later were transduced with MSCV–Bcl-x_L by spin inoculation as described above. Following incubation for 1 h at 37°C, cells were collected, resuspended in pre-B cell medium, and then cultured for an additional 48 h. Cells were then infected at a high multiplicity of infection (MOI) with MIT or MIT-Cre. Culture was continued with IL-7 for 3 days and then collected for PCR and reverse transcription-PCR (RT-PCR) experiments.

Inducible shRNA silencing of BCL11A. Two complementary short hairpin RNA (shRNA) template oligonucleotides targeting exon 2 of BCL11A were synthesized and cloned into the pRSMX-PG vector (5) using HindIII and BglII sites. pRSMX-PG-BCL11A-shRNA retrovirus was produced in Phoenix cells as described above and used to infect a Tet-on human B cell line, BJAB (38), which expresses the Tet repressor. Transduced BJAB cells were selected in the presence of puromycin for 6 days. BCL11A-specific shRNA expression was induced with different concentrations of doxycycline, and samples were tested at regular intervals for 48 h. Levels of BCL11A expression were measured by RT-PCR and Western blot analysis. The following oligomers were used for the BCL11A shRNA template: 5′-GATCACCCCAGCACTTAAGCAAATTCAAGAG ATTTGCTTAAGTGCTGGGGTTTTTTTGGAAA-3′ (forward) and 5′-A GCTTTTCCAAAAAAACCCAGCACTTAAGCAAATCTCTTGAATTT GCTTAAGTGCTGGGGTG-3′ (reverse). BglII and HindIII sites were used for cloning.

Plasmid constructions. pCMV10–BCL11A-XL and pCMV10–BCL11A-S were constructed as follows: BCL11A-XL and BCL11A-S were amplified by PCR with the same forward primer, 5′-GCCAAAGCTTAT GTCTCGCCGCAAGCAAGGC-3′, and different reverse primers, 5′-CCCAGGATCCTATTCAGTTTTTATATCATTATTCAAC-3′ for the BCL11A-XL isoform and 5′-CCCAGGATCCTCAAATTTTCTCAGAAC TTAAG-3′ for the S isoform. The PCR products were digested with BamHI and HindIII and cloned into pCMV10 (Sigma), which contains a sequence of 3× Flag tag. The pXY-BCL11A-XL plasmid was constructed by using pCMV10–BCL11A-XL as a template and the following PCR primers: 5′-CCGGGATCCATGGACTACAAAGACCATGAC-3′ (forward) and 5′-GGACGCGGCCGCTATTCAGTTTTTATATCATTATT C-3′ (reverse). The PCR products were digested with BamHI and NotI and cloned into the pXY-IRES-puro plasmid using BglII and NotI sites. pEGFPC1-BCL11A and BCL11A-XL-K5N were generated by site-directed mutagenesis using the QuikChange site-directed mutagenesis kit and protocol from Stratagene. The following primers were used: 5′-CCA TGTCTCGCCGCAACCAAGGCAAACCCCCAGC-3′ (forward) and 5′-GCTGGGGTTTGCCTTGGTTGCGGCGAGACATGG-3′ (reverse). The deletion mutant pEGFPC1-BCL11ABCL11A-XLdelN80 was constructed by using PCR with the following primers: 5′-GGCGTCGACAGCGAAC ACGGAAGTCCC-3′ (forward) and 5′-CCCAGGATCCTATTCAGTTT TTATATCATTATTCAAC-3′ (reverse). The PCR products were digested by using SalI and BamHI and cloned into the plasmid vector pEGFPC1. The final clones were verified by sequencing.

ChIP and EMSA. Chromatin immunoprecipitation (ChIP) was performed according to instructions provided with the Upstate ChIP kit. Human pre-B and B cell lines (Nalm6 and Raji) were cross-linked by incubation at room for 8 min in a final concentration of 1% formaldehyde. Fixed cells were washed twice with ice-cold phosphate-buffered saline (PBS) and lysed in SDS lysis buffer (1% SDS, 10 mM EDTA, and 50 mM Tris [pH 8.1]). Lysates were sonicated for 0.5 min six times to a modal distribution of ~1,000 bp. Sonicated chromatin was diluted 10-fold in a dilution buffer (0.01% SDS, 1.1% Triton X-100, 1.2 mM EDTA, 16.7 mM Tris-HCl [pH 8.1], 167 mM NaCl) and then immunoprecipitated with purified rabbit IgG or with an anti-BCL11A-XL specific rabbit polyclonal antibody (BL1797; Bethyl). Antibody-chromatin complexes were washed with a low-salt wash buffer (0.1% SDS, 1% Triton X-100, 2 mM EDTA, 20 mM Tris-HCl [pH 8.1], 150 mM NaCl), a high-salt wash buffer (0.1% SDS, 1% Triton X-100, 2 mM EDTA, 20 mM Tris-HCl [pH 8.1], 500 mM NaCl), an LiCl wash buffer (0.25 M LiCl, 1% IGEPAL CA-630 [octylphenoxypolyethoxyethanol], 1% deoxycholic acid [sodium salt], 1 mM EDTA, 10 mM Tris [pH 8.1]), and a TE wash buffer (10 mM Tris-HCl [pH 8.0], 1 mM EDTA). These complexes were eluted in elution buffer (1% SDS, 0.1 M $NaHCO_3$) and reverse cross-linked at 65°C for 6 to 12 h in the presence of 0.2 M NaCl. After proteinase K treatment for 1 h at 45°C, DNA was recovered by using PCR purification columns (Invitrogen) and then used for PCR analysis. The *RAG1* and *RAG2* promoters and the *Erag* enhancer region were detected by using the following primers: RAG1 forward primer 5′-CATTCTCAGGGAGGGAACTG-3′, RAG1 reverse primer 5′-GGAGGGCTAACCACAAATGA-3′, RAG2 forward primer 5′-GTGGTCTCTGCTTCAGGACA-3′, RAG2 reverse primer 5′-AGCAACA ATGGCAACACAAT-3′, Erag forward primer 5′-GCACTGCAAATGGC CTGTGAAC-3′, and Erag reverse primer 5′-GAGACCAGAGGGCTTAA CATTG-3′. ChIP-PCR of RAG1, RAG2, and Erag produced 161-bp, 180-bp, and 196-bp products, respectively. Thermal cycling conditions were 95°C for 5 min and then 35 cycles at 95°C for 10 s, 55°C for 15 s, 72°C for 10 s, and 72°C for 7 min. PCR conditions used for the *Erag* enhancer were 95°C for 5 min and then 35 cycles at 95°C for 1 min, 57°C for 1 min, 72°C for 1 min, and 72°C for 7 min.

To construct electrophoretic mobility shift assay (EMSA) probes, the proximal promoter region (243 bp upstream of the transcriptional start site [TSS] [−243] to 123 bp downstream of the TSS [+123]) of the mouse *RAG1* gene (39) was amplified by PCR using RAG1 forward primer 5′-C ATTCTCAGGGAGGGAACTG-3′ and RAG1 reverse primer 5′-GGCAA AGTGTGTTCTCTGCTC-3′ from plasmid template R1P-Luc. The *Erag* enhancer (10) probe was a 196-bp fragment extending from the KpnI site to the end of region A (11). The probe for the distal promoter region of *Rag1* (positions −713 to −563) was generated by KpnI-HindIII digestion of plasmid −713-R1P-Luc. Probes were end labeled with ^{32}P by using polynucleotide kinase and then purified by using Bio-Spin columns (Bio-Rad) and 6% native gels. Reaction mixtures consisted of 5 to 10 μg of nuclear extract prepared from various B cell lines, probes, and a binding buffer (20 mM HEPES [pH 7.9], 40 mM KCl, 6 mM $MgCl_2$, 1 mM dithiothreitol [DTT], 0.1% NP-40, 3 mg/ml bovine serum albumin, 10% glycerol, 2% Ficoll, 50 μg/ml of sonicated salmon sperm DNA, and protease inhibitor cocktail). The binding mixture was incubated at room temperature for 30 min. For the antibody binding competition assays, 100 ng of BCL11A polyclonal antibody (BL1797) or of monoclonal antibody (MAb) mAb123 (40) or an equal amount of a control rabbit IgG antibody or an irrelevant tubulin MAb was added at the initiation of each binding reaction. Cold competitions were carried out with increasing molar ratios of wild-type (5′-GGTCAGTCCGTTTCCAACTTCCTCCAGCAG-3′) and mutant (5′-GGTCAGTCCGTGGGTAAGCCCCTCCAGCAG-3′) duplexed, gel-purified oligonucleotides spanning the putative BCL11A binding site at *Erag* nucleotide (nt) positions 121 to 131. (Mixtures were fractionated on 6.0 to 7.5% nondenaturing acrylamide. The gels were dried and analyzed by using a PhosphorImager [Molecular Dynamics].)

Luciferase assays. Pre-B cells (A70, A70-BCL11A-XL, and A70-BCL11A-XL-K5/A) and non-B cells (293T, COS-7, and NIH 3T3) were plated at ~1 ×10^6 cells per well in 12-well plates. Twenty-four hours later, pre-B cells were transiently transfected with 1 μg of firefly luciferase reporters (detailed in Fig. 6), 5 ng of *Renilla* luciferase, and, in some cases, 1 μg of pFLAG-MTA1 using the mouse B cell Nucleofector kit (VPA-1010, program Z-01) and cell line kit (VCA-1003, program M13) according to the manufacturer's recommended protocol. The transfection efficiency (determined by pEG-GFP transfection in parallel assays) achieved in pre-B cells was 40 to 50%. Empty vector plasmid DNA was used to keep the total amount of transfected DNA equal under each experimental condition.

Non-B cells were transiently transfected with 1 μg of the firefly luciferase reporter constructs (detailed in Fig. 6), 5 ng of *Renilla* luciferase, and either wild-type BCL11A-XL or BCL11A-XL-K5/A expression vectors over a concentration range of 0.1 to 1.5 ng. An empty pCMV10 construct

was then added to each transfection mix to ensure that final DNA concentrations were equal.

Forty-eight hours after transfection, cells were harvested for dual-luciferase reporter assays (Promega), using cell lysis and luciferase measurements as described in the manufacturer's manual. Values were normalized by determining the ratio of firefly to *Renilla* luciferase for each transfection. To determine fold expression, the firefly/*Renilla* ratio in experimental samples (i.e., those with BCL11A-XL overexpression, the *Renilla* vector, and its respective firefly luciferase RAG reporter) was compared to the firefly/*Renilla* ratio from basal luciferase expression samples (i.e., those without BCL11A-XL overexpression). Western blotting confirmed that BCL11A-XL protein lysate levels corresponded to the concentration of input DNA.

Microarray. Briefly, 3 μg of mRNA of various human pre-B and B cell lines was reverse transcribed by using aminoallyl UTP/deoxynucleoside triphosphates (dNTPs). Synthesized cDNA was hydrolyzed and column purified (Invitrogen). Each cDNA sample was coupled with cy3 or cy5 dye, mixed, and hybridized to full genome human array slides. Microarray slides were scanned by using a GenePix 4000a microarray scanner.

Flow cytometry. A70-INV and A70-INV-BCL11A-XL cells were incubated in the absence or in the presence of 3 μM STI571 (Novartis) for 3 days. The harvested cells were washed two times with ice-cold PBS and resuspended in PBS at a concentration of $\sim 1 \times 10^6$ cells/ml. A minimum of 5,000 cells per sample was used for each analysis. Flow cytometry (BD FACSCalibur flow cytometry system) was used to analyze the samples for green fluorescent protein (GFP)-positive signals. Cell debris and dead cells were excluded from the analysis by forward- and side-scatter analysis. The parental A70-INV cells were used for GFP gating. Data were analyzed by using Cell Quest software. *Bcl11a*$^{L/L}$/MIT and *Bcl11a*$^{L/L}$/MIT cultured bone marrow cells were costained under similar conditions and stained with fluorescein isothiocyanate (FITC)-conjugated anti-Thy-1.1 (T1-A3; Abcam) and *R*-phycoerythrin-conjugated anti-B220 (RA3-6B2; BD Pharmingen). For DNA content/cell cycle analysis, cells were incubated for 15 min at 20°C in 300 to 500 μl propidium iodide–Triton X-100 staining solution (catalog number 11348639001; Roche). Data were acquired as described above.

Genomic DNA isolation and Southern blotting. A DNeasy tissue kit (Qiagen) was used to isolate genomic DNA from cultured A70-INV cells or bone marrow-derived B220$^+$ pre-B cells according to previously reported protocols, with some modifications (39, 41). For genomic PCR, 100 to 200 ng of genomic DNA was PCR amplified and then subjected to electrophoresis in agarose gels. The scheme for detected inversion of the ectopic locus by GFP flow cytometry or by PCR is illustrated in Fig. 5C. PCR products were transferred onto a nylon membrane for Southern blot analysis. A Jκ2-2 oligonucleotide probe was end labeled with T4 polynucleotide kinase. Southern blots were prehybridized overnight and then hybridized with probes for 3 h at 50°C in Ultra-hyb solution (Ambion). Blots were washed once at room temperature and twice at 50°C in 2× SSC (1× SSC is 0.15 M NaCl plus 0.015 M sodium citrate)–0.1% SDS for 30 min each, and signals were detected by using a PhosphorImager (Molecular Dynamics). The following primers were used for PCR detection of inversion: 5′-CACAACATCGAGGACGG-3′ (pA) and 5′-GCACCACTTTCTTTCCCTGA-3′ (hCD4R). The primers for endogenous rearrangement and blotting were as follows: Vcon forward primer 5′-CCGAATTCGSTTCAGTGGCAGTGGRTCWGGTAC-3′, Jκ2-1 reverse primer 5′-GGTTAGACTTAGTGAACAAGAGTTGAGAA-3′, Jκ2-2 probe 5′-CAAGAGTTGAGAAGACTACTTACGTTTT-3′, and Jκ2-2 reverse primer 5′-TGCCACGTCAACTGATAATGAGCCCTCTC-3′. The amplification conditions were 30 cycles at 94°C, 90 cycles at 60°C, and 60 cycles at 72°C.

Semiquantitative RT-PCR. RNA purification was performed with TRIzol LS according to the manufacturer's instructions (Invitrogen). Pellets were resuspended in RNase-free water. For first-strand synthesis by reverse transcription, we used the SuperScript II First kit (Invitrogen). Serial dilutions of template cDNA were subjected to 30 cycles of PCR by using amplification conditions reported previously (7, 8, 11, 14, 15, 19, 30).

Quantitative PCR. Either genomic DNA or cDNA transcribed with the SuperScript RT III-based protocol mentioned above was analyzed by quantitative real-time PCR performed on an Applied Biosystems ViiA7 thermocycler using Sybr green chemistry (Applied BioSystems Sybr green or Quantus Sybr green). All assays were performed in triplicate and analyzed by the standard curve method with normalization to the housekeeping gene glyceraldehyde-3-phosphate dehydrogenase (GAPDH) (42, 43).

Oligonucleotide primers. Primers used for semiquantitative and quantitative PCR (in the 5′-to-3′ orientation) were as follows: RAG1-F (CCAAGCTGCAGACATTCTAGCACTC), RAG1-R (CTGGATCCGGAAAATCCTGGCAATG), RAG2-F (CACATCCACAAGCAGGAAGTACAC), RAG2-R (GGTTCAGGGACATCTCCTACTAAG), IRF4-F (CCACGGACACACCTATGATG), IRF4-R (GGTCTGGAAACTCCTCACCA), IRF8-F (GGGCTGCCTAAGTTGTATG), IRF8-B (ACCACCCTGCTGTCAGGTAG), Spi-B-F (GAGGACTTCACCAGCCAGA), Spi-B-R (TGAGTTTGCGTTTGACCTTG), gVk-F (CCACATGCCTTTCTTCAGGGACAAGTG), gVk-R (TTATGTCGTTCATACTCGTCCTTGGTC), Foxp1-F (AAGGGGCAGTATGGACAGTG), Foxp1-R (CCCAGAGGTTCACTCCATGT), BCL11A-F (CCCAGAGTAGCAAGCTCACC), BCL11A-R (CAGGATCCTATTCAGTTTTTATATCATTATTC), FoxO1-F (CAAAGTACACATACGGCCAATCC), FoxO1-R (CGTAACTTGATTTGCTGTCCTGAA), E2A-F (TTGTGGACATTTTCTAGGCAG), E2A-R (ATGTGTGGTGGCCCACACTTG), Pax5-F (AGACAGGAAGCATCAAGCCTG), Pax5-R (CAGCGAGGCCATGGCTGAATA), Vpre-B-F (GTAGAGGCATGCCAGCCGGTGCT), Vpre-B-R (CTTGAAGCTTTCGAGGGACACGTGT), λ5-F (ACTGTCGGATCCTCGCAGAGCAGG), λ5-R (CAGTCAAGCTTCTATGAACATTCT), GAPDH-F (ACTTTGTCAAGCTCATTTCC), GAPDH-R (TGCAGCGAACTTTATTGATG), VCON-F (CCGAATTCGSTTCAGTGGCAGTGGRTCWGGTAC), and Jκ2-1-R (GGTTAGACTTAGTGAAGAGTTGAGAA).

Biochemistry. Western blotting was carried out as previously described (30). The following dilutions were used for each antibody: 1:5,000 for Flag (Sigma), 1:2,000 for β-tubulin (Santa Cruz), 1:2,000 for RAG1 (catalog number 554116; Pharmingen), 1:3,000 for BCL11A-XLc (BL1797; Bethyl), 1:2,000 for BCL11A-mAB123 (prepared in our laboratory), 1:1,000 for lamin B (Santa Cruz), and 1:1,500 for cytochrome *c* (catalog number 556432; Pharmingen).

Nuclear subcellular fractionation was carried out with a minor modification (9) of a procedure described previously by Reyes et al. (44). Cytoplasmic contamination into the nuclear fraction will result in contamination within the soluble NP fraction (2). Lamin B signals were used to evaluate contamination of nuclear fractions into the cytoplasmic fractions (44). Cytoplasmic contamination was also assessed by anti-cytochrome *c* Western analysis.

RESULTS

BCL11A-XL modulates RAG expression. As an initial approach, we used microarrays to identify genes that are deregulated by BCL11A-XL overexpression in mature B (Raji, Ramos, OCI-LY7, and BJAB) and pre-B (NALM6) human cell lines. B cell lines were transduced with pXY-puro (mock control) or with the same virus containing an N-terminally Flag-tagged, full-length BCL11A-XL cDNA. Among the 17,856 clones tested, 43 clones, which represent 39 genes, showed alterations of at least 2-fold in all four cell lines. As expected from previous studies of BCL11A function, most of the transcripts were downregulated (data not shown). Among the 11 upregulated genes, *RAG1* was consistently observed, even though the basal transcript levels in the mature lines were near baseline (Fig. 2A).

We created a stable BCL11A-XL-overexpressing line of NALM6 pre-B cells and checked *RAG1* and *RAG2* expression by semiquantitative RT-PCR. As shown in Fig. 2B, both *RAG* genes

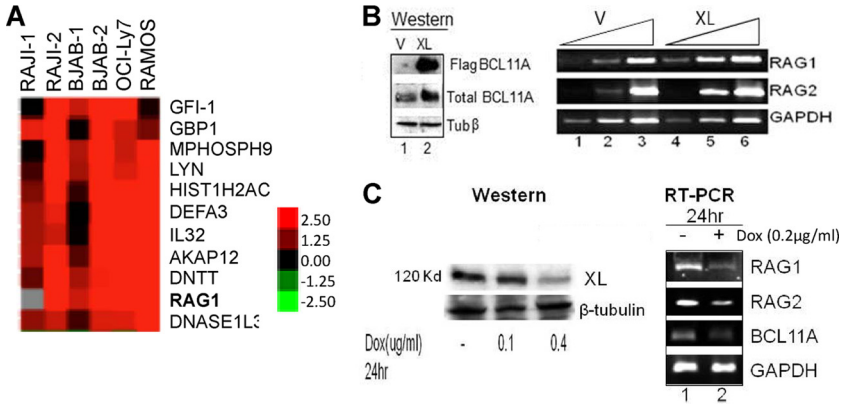

FIG 2 BCL11A-XL regulates RAG expression. (A) Microarray identification of RAG1 upregulation. The indicated human B cell lines were stably transduced with a BCL11A-XL (XL) retrovirus or with the pXY-puro empty vector. Expression profiling was performed in multiple ($n > 4$) independent experiments tracked by multiple probe elements spotted per microarray. Shown are the 11 transcripts upregulated by minimally 2-fold relative to the vector control in all cell lines. (B) Overexpression of BCL11A-XL upregulates RAG. Human NALM6 pre-B cells were stably transduced with BCL11A-XL or the pXY-puro virus control (V). (Left) Western blot in which Flag-BCL11A indicates anti-Flag detection of viral BCL11A-XL expression. Total BCL11A, anti-BCL11A-XL MAb detection; Tubβ, anti-β-tubulin control. (Right) RT-PCR demonstrates upregulation of RAG1 and RAG2. Serial template dilution (3-fold) (indicated by triangles) confirmed that RT-PCR was semiquantitative. GAPDH was used as a loading control. (C) Inducible shRNA knockdown of BCL11A-XL reduces RAG expression. BJAB B cells were stably transduced first with a retrovirus expressing the bacterial tetracycline repressor (TETR) and the blasticidin resistance gene and then with a pRSMX-PG retrovirus containing shRNA targeted to exon 2 of BCL11A-XL under the control of a modified H1 promoter containing binding sites for the tetracycline repressor (38). Significant downregulation of BCL11A-XL protein (left) and transcript (right) with concomitant downregulation of RAG1 and RAG2 was observed 24 h following addition of the tetracycline analogue doxycycline (Dox).

were significantly upregulated. As a complementary approach, inducible short hairpin RNA (shRNA) interference was used to specifically target a region (exon 2) common to all BCL11A isoforms. As shown in Fig. 2C, we observed a robust knockdown of *BCL11A* transcripts as well as a corresponding reduction in both RAG1 and RAG2 transcripts by the end of the first 24 h of induction.

BCL11A is recruited to the *RAG1* promoter and to the *Erag* enhancer *in vivo* and *in vitro*. Chromatin immunoprecipitation (ChIP) was employed to test whether BCL11A-XL is recruited to the *RAG* promoters or *RAG* enhancer loci in human pre-B cell (NALM6) and mature B cell (Raji) chromatin. Specific sets of primers were designed within the upstream 1-kb region of each promoter and within the ~0.8-kb first one-third of the *Erag* enhancer. ChIP-PCR demonstrated that the *RAG1* promoter and *Erag*, but not the *RAG2* promoter or the *Ep* or *Ed* enhancer, were enriched in pulldowns with anti-BCL11A but not with control antibody (Fig. 3A and data not shown). This indicated that BCL11A-XL is recruited either directly or indirectly to the proximal promoter of *RAG1* and to the *RAG* enhancer *in vivo*.

EMSAs were performed to validate and extend the results shown in Fig. 3A. A ^{32}P-labeled 196-bp probe extending from the 5′ end to the 3′ end of region A of *Erag* (11) was incubated with nuclear extracts prepared from Raji B cells, and several complexes were observed (Fig. 3B). A slowly migrating species (boxed in Fig. 3B to E) was specifically abolished by pre- or postincubation with anti-BCL11A monoclonal antibody (Ab123) or a polyclonal antibody specific for the BCL11A-XL C terminus (Fig. 3B, lanes 3 and 5) but not with control antibodies (Fig. 3B, lanes 4 and 6). Specific double-stranded-oligonucleotide competition (Fig. 3B, compare lanes 8 to 10 to lanes 11 and 12) identified a BCL11A binding site that closely matched (8/10) the BCL11A consensus determined by high-resolution, genome-wide ChIPseq derived publically from the human B cell lymphoma GM12728 (28) (Fig. 3F). This site is overlapped from positions −2 to +4 with a consensus binding site (GAGGAA) for PU.1, an essential myeloid/lymphoid transactivator, which was shown to bind to the *Ep* element (Fig. 1A) (16). Accordingly, we observed partial ablation of the BCL11A complex with anti-PU.1 (Fig. 3B, lane 7), suggesting that these factors might act in concert or in opposition at this apparent composite site. Using a similar approach with nuclear extracts prepared from pre-B (NALM6) (Fig. 3C, lanes 2 to 7), pro-B (HAPTL1) (Fig. 3C, lanes 8 to 13, and D, lanes 2 to 10), and mature B (Raji) (Fig. 3C, lanes 14 to 19, and E, lanes 2 to 4) cell lines, we validated two similarly migrating BCL11A complexes within the distal (nt −426 to −416) and proximal (nt −207 to −197) regions of the *RAG1* promoter (Fig. 3C to E). Ablation as opposed to supershifting of complexes suggested that both anti-BCL11A antibodies interfere with DNA binding, leading to dissociation of BCL11A-DNA complexes. Both proximal and distal BCL11A-XL binding sites are well within the ChIP region shown in Fig. 3A. Further consistent with our ChIP-PCR results, no binding to *RAG2* promoter probes was observed (data not shown), nor did we detect specific binding when recombinant, *in vitro*-translated BCL11A-XL, -L, or -XS was employed in the EMSAs (data not shown). This suggested that BCL11A-XL binding requires a complex provided by another factor(s), potentially PU.1, present in nuclear extracts in pro-B, pre-B, and mature B cells.

BCL11A-XL transactivates *RAG1* and *Erag-RAG2* transcription in pre-B cells. Transformation of murine fetal liver or bone marrow B cell progenitors by the Abelson murine leukemia virus arrests cells at the early (large) pre-B cell stage with low to negligible Rag1 and Rag2 expression levels (6). One such line, A70 (39), expresses negligible levels of BCL11A (Fig. 4A) and was employed for functional evaluation of *Rag* activation. Stable BCL11A-XL overexpression, achieved by retroviral transduction, induced high levels of endogenous *Rag1* and *Rag2* (Fig. 4A). These cells (termed A70-BCL11A-XL) were compared to the parental BCL11A-XL-negative A70 line following transient transfection with luciferase

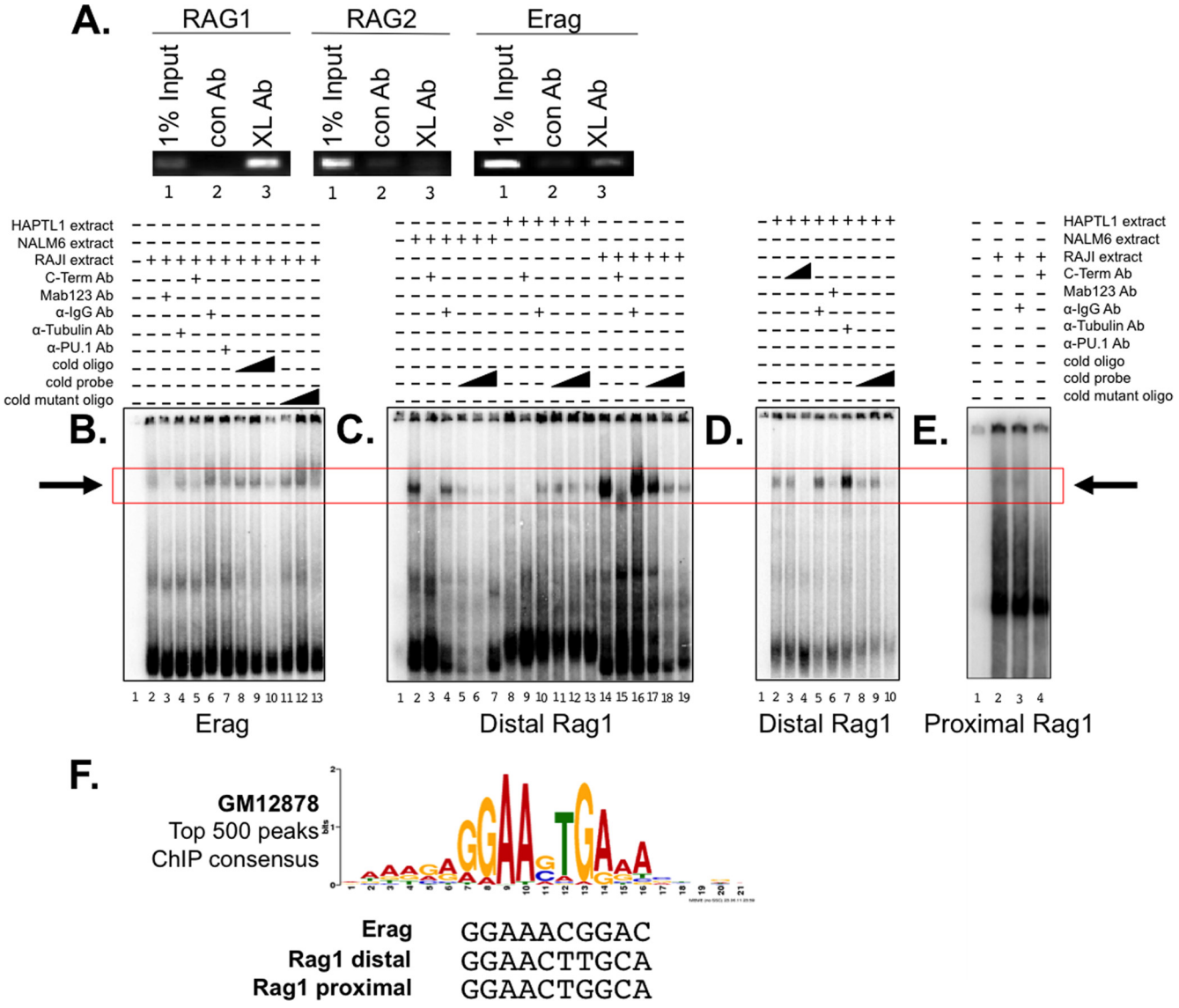

FIG 3 BCL11A is recruited to the *RAG1* promoter and the *Erag* enhancer *in vivo* and *in vitro*. (A) ChIP-PCR identifies the *RAG1* promoter and *Erag* enhancer as targets for BCL11A binding. A rabbit polyclonal antibody (BL1797; Bethyl) specific to the BCL11A-XL C terminus (BCL11A-XL Ab) was used to immunoprecipitate NALM6 pre-B cell chromatin. The samples were reverse cross-linked, purified, and analyzed by semiquantitative PCR using primers that amplify regions within the proximal *RAG1* and *RAG2* promoters and within the *Erag* enhancer. Specific enrichment was observed for the *RAG1* promoter and the *Erag* enhancer (lanes 3 and 9) but not for the *RAG2* promoter (lane 6). PCRs from 1% input were used as positive controls (lanes 1, 4, and 7). Purified rabbit IgG antibodies (con Ab) did not immunoprecipitate target DNA significantly (lanes 2, 5, and 8). (B) BCL11A binds to the *Erag* enhancer *in vitro*. A 196-bp probe extending from the 5′ boundary (KpnI site) to the end of region A of *Erag* (11) was labeled with ^{32}P and then incubated with nuclear extracts prepared from the Raji B cell line. Specificity of binding was tested by further incubation of the indicated probe-nuclear extract mixtures with anti-BCL11A-XL (BL1797) C-terminal polyclonal antibody (C-Term Ab), with monoclonal antibody (mAb123 Ab), with monoclonal anti-PU.1 antibody (α-PU.1), or with control polyclonal (α-IgG Ab) and monoclonal (α-Tubulin Ab) antibodies employed at the same concentrations. Cold competitions employed double-stranded 30-mers of wild-type (cold oligonucleotide) and mutated (cold mutant oligonucleotide) oligonucleotides spanning the putative BCL11A binding site at nt 121 to 131. Triangles represent molar excesses of 10-, 50-, and 100-fold relative to labeled probe. Complexes were resolved on native 6% gels, with specific binding highlighted by boxes. (C and D) BCL11A binds to a consensus site within the distal region (positions −426 to −416) of the *RAG1* promoter. The probe was a 300-bp KpnI-XhoI fragment. (E) BCL11A binds to a consensus site within the proximal region (positions −207 to −197) of the *RAG1* promoter. The probe was a 263-bp PCR product spanning positions −228 to +35. (F) Alignment of BCL11A binding sites determined in this study with consensus of the top 500 peaks determined by ENCODE ChIPseq in GM12878 human B cell lymphoma (28).

(Luc) reporter constructs that were previously shown (10, 17) to recapitulate authentic activities of the proximal *Rag1* (−243-R1p-Luc) and *Rag2* (−279-R1p-Luc) promoters in the absence or presence of the full 2.3-kb *Erag* enhancer. A70-BCL11A-XL firefly luciferase activities were normalized relative to cotransfected *Renilla* luciferase activities and plotted as fold activation over a promoterless luciferase control.

As shown in Fig. 4B, BCL11A-XL only modestly increased *Rag1* proximal promoter-driven transcription levels (average, 1.6-fold). Appending *Erag* to the reporter provided an ~4-fold en-

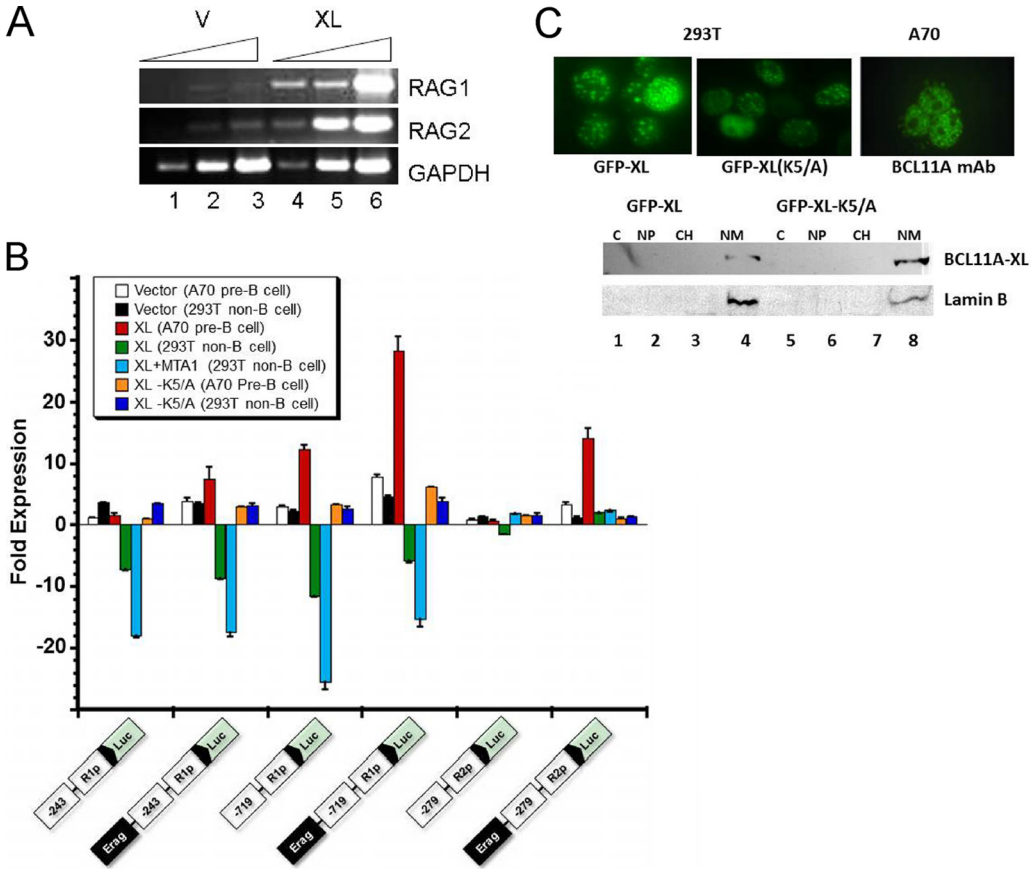

FIG 4 RAG transcriptional reporter activity is activated in pre-B cells but repressed in non-B cells following BCL11A-XL overexpression. (A) Establishment of stable overexpression. A70 pre-B cells were transduced with pXY-IRES-puro (V) or pXY-BCL11A-XL (XL) and selected with 1 μg/ml of puromycin for 6 days. Triangles represent 5-fold dilutions of cDNA. (B) BCL11A-XL transactivates *RAG1* promoter-driven and *Erag-RAG2* promoter-driven transcription in A70 pre-B cells but represses RAG promoter-driven activity in 293T epithelial cells. A70 and 293T cells, stably transduced with pXY vector only (V), BCL11A-XL, or BCL11A-XL mutated at an essential N-terminal K5 (XL-K5/A), were transiently transfected, as described in Materials and Methods, with the indicated firefly luciferase constructs and a *Renilla* luciferase control. Cells were harvested 40 to 48 h later, and firefly luciferase values were normalized to *Renilla* luciferase values. The ratio is expressed as fold changes by arbitrary assignment of a value of 1.0 for the empty vector (pXY-IRES-puro for pre-B cells or pCMV10 for non-B cells). Fold changes are plotted on the *y* axis, with the magnitude of activation denoted by increasing positive values and repression indicated by negative values. Error bars indicate standard deviations of 3 to 5 independent experiments. (C) Wild-type BCL11A-XL and the BCL11A-K5/A mutant localize indistinguishably within the nuclear matrix of paraspeckles in pre-B and non-B cells. (Top) Fixed amounts of GFP–BCL11A-XL and GFP–BCL11A-XL-K5/A were imaged following transient transfection into 293T cells. Ectopically transduced A70-BCL11A-XL cells were stained with anti-BCL11A monoclonal antibody Ab123. (Bottom) Biochemical fractionation of transiently transfected 293T cells with the indicated wild-type or mutant BCL11A-XL constructs. Equivalent amounts of cytoplasmic (C), soluble nuclear (NP), chromatin (C), and nuclear matrix (NM) fractions were fractionated (44) on SDS-PAGE gels and then Western blotted with antibodies specific for BCL11A or for the nuclear matrix marker lamin B.

hancement in A70, which was doubled in the A70-BCL11A-XL transductants. When the *RAG1* promoter was extended to include the more distal BCL11A-XL binding region located at position ~−640 (−719-R1p-Luc), we observed an ~3-fold increase above the levels observed for the proximal *Rag1* promoter alone and an ~12-fold increase in the presence of *Erag*. Consistent with the EMSA and ChIP data, no effect of BCL11A-XL overexpression on *Rag2* proximal promoter-luciferase activity alone was observed. However, inclusion of *Erag* on the construct resulted in an ~3-fold increase in the absence of BCL11A-XL and an ~14-fold increase in *Rag2* reporter activity in the presence of BCL11A-XL overexpression (Fig. 4B).

The N termini of several members of the BCL11A superfamily (30) constitute the transactivation domain, and K5 was shown to be essential in several cases (26, 45) (Fig. 1B). Activation of all reporter activities by BCL11A-XL was abrogated by the K5/A substitution (Fig. 4B). Collectively, the data indicate that BCL11A-XL acts at the *Rag1* promoter, primarily through a distal binding site, whereas BCL11A-XL activates *Rag2* transcription exclusively via *Erag* binding.

Enforced expression of BCL11A in non-B cells represses RAG1-mediated transcription. The above-described results, along with the PU.1 DNA binding cooccupancy implications of Fig. 3 and previous observations that RAG1 expression is not lymphoid restricted (9, 12), prompted us to test the cell type specificity of BCL11A-mediated RAG transactivation. Contrary to what was observed for pre-B cells, BCL11A-XL overexpression in 293T cells led to strong repression (~5- to 6-fold) of both proximal (−243-R1p) and distal (−719-R1p) *Rag1* promoter-driven activities, whereas *RAG2* and *Erag-RAG2* luciferase activities were unaffected (Fig. 4B). This indicated that the more proximal BCL11A binding site within the *Rag1* promoter is sufficient for targeting

maximal repression. Similar results were observed for additional non-B cell lines (NIH 3T3, COS-7, and HeLa) and were confirmed by careful dose-response curves following transient cotransfection (data not shown).

BCL11B, the highly similar paralogue of BCL11A (23), was shown to interact with the nucleosome-remodeling and histone deacetylase (NuRD) complex with enhanced repression of model substrates (46). One of the NuRD components, metastasis tumor antigen 1 (MTA1), was shown to interact with and enhance BCL11B repression synergistically, while MTA2 had no effect (46). We observed significant augmentation of BCL11A-XL repression following cotransfection with MTA1 (Fig. 4B) but not with MTA2 (data not shown). Conversely, enforced overexpression of BCL11A-XL with MTA1 in A70 pre-B cell lines had no effect on activation of any of the *Rag1* or *Rag2* constructs (data not shown).

We considered, as an alternative explanation for the opposite effects in B versus non-B cells (other than B-lineage-specific cofactors), a differential subcellular localization of BCL11A-XL. In B cells, exogenous or ectopically overexpressed BCL11A-XL accumulates primarily within the nuclear matrix of paraspeckles (30). We observed localization indistinguishable from that following ectopic delivery of GFP–BCL11A-XL or GFP–BCL11A-XL-K5/A into 293T cells (Fig. 4C, top). Biochemical subcellular fractionations (Fig. 4C, bottom) indicated that, as in B cells (30), wild-type and mutant BCL11A-XL accumulate preferentially within the nuclear matrix.

The results suggest that BCL11A-XL acts in a context-dependent, cell-type-specific mode to activate or repress *RAG1* transcription. The data further suggest that repressive BCL11A-XL complexes differ from activation complexes by the inclusion/exclusion of the MTA1 corepressor but are indistinguishable in their subcellular localization.

BCL11A-XL induces ectopic V(D)J recombination in A70-INV pre-B cells. The A70-INV Abl-transformed pre-B cell line retains the properties of the parental A70 cell line, but it has been engineered for inducible V(D)J recombination analysis by integration of a recombination substrate, pMX-INV, which, upon inversion, activates expression of GFP (39). A70 and A70-INV also constitutively express a *Bcl2-Eμ* transgene, enabling them to survive apoptotic signaling for several days (39). We transduced A70-INV cells with empty virus (pXY-puro) or with pXY-BCL11A-XL and then puromycin selected bulk (uncloned) cells. As with A70 parental cells, BCL11A protein was barely detectable in untransduced or mock-transduced A70-INV cells (Fig. 5A). Transduced cells expressed significant levels of BCL11A-XL, resulting in robust induction of Rag1 and Rag2 (Fig. 5B).

The strategy used to detect the inversion of pMX-INV and V-J recombination of the endogenous κ light chain locus was described previously (39) (Fig. 5C). As a positive control, strong induction of recombination is achieved by treatment of A70-INV cells with the Abl kinase inhibitor STI571 (47). STI571 causes differentiation of early pre-B cells to a late-pre-B-cell-like state (47). Strong Rag1 and Rag2 expression ensues, followed by Vκ-Jκ recombination and, in A70-INV cells, inversion of the integrated pMX-INV via cleavage at the flanking recombination signal sequences (RSSs) (Fig. 5C) (39). As shown in Fig. 5D, mock viral transduction produced 0.7% and 18.1% GFP-positive cells without or with STI571 treatment, respectively (Fig. 5DA and B). This level of background GFP expression is similar to previously reported data (39). BCL11A-XL-infected cells produced 7% and 34.5% GFP-positive cells without or with STI571 treatment, respectively (Fig. 5DC and DD).

An ~10-fold increase in recombination substrate inversion by BCL11A-XL in the absence of STI571 treatment suggested that BCL11A-XL acts independently. Consistent with this interpretation, the level of substrate inversion by BCL11A-XL in the presence of STI571 was additive. Unlike the G_1/S arrest induced by STI571 treatment, BCL11A-XL transduction was accompanied by no alteration in cell cycling (as measured by DNA content of propidium iodide-stained cultures [data not shown]).

To verify that GFP expression resulted from inversion of pMX-INV, we carried out semiquantitative PCR on genomic DNA using a 3′ primer complementary to hCD4, a component of the PMX-INV vector which can be used to detect inverted GFP. pMX-INV inversion allows successful PCR product formation by providing the reverse primer with the correct orientation of GFP cDNA (Fig. 5C). As shown in Fig. 5E, an increase in the intensities of inverted GFP-hCD4 PCR products was observed in STI571-treated or BCL11A-XL-transduced cells compared to STI571-untreated or mock virus-transduced cells.

Modulation of BCL11A expression in transformed or normal murine pre-B cells modulates endogenous V(D)J recombination. Although integrated as a single copy, the pMX-INV reporter locus may not display the equivalent heterochromatin structure as the endogenous light chain loci in pre-B cells. To assess whether the endogenous locus can also be induced to rearrange by BCL11A-XL overexpression, genomic DNA was analyzed by PCR using a "universal" Vκ forward primer and Jκ2-1 reverse primer (Fig. 6A, top). Efficient PCR can occur only if VJκ rearrangement deletes the intervening sequence between Vκ and Jκ elements. VJκ rearrangement was evaluated by Southern blotting with a Jκ2-2 oligonucleotide probe (Fig. 6A). As shown in Fig. 6A (bottom), increased levels of Jκ rearrangement were observed in both STI571-treated (lanes 4 to 6) and BCL11A-XL-transduced (lanes 10 to 12) cells compared to control cells.

To address the issue in normal developing B cells, we employed mice with *loxP* (*L*) sites flanking exon1 of the *Bcl11a* gene (*Bcl11a*$^{L/L}$) (29, 35; Ippolito et al., submitted). Bone marrow cultures were established as previously described (8, 36), by expanding bead-purified B220$^+$ cells in culture with IL-7. In an effort to delete *Bcl11a*, the cells were infected with either an empty vector (MIT [mouse stem cell virus–internal ribosomal entry site–Thy-1.1]) or the equivalent retrovirus which expresses Cre recombinase (MIT-Cre). Within 3 days, the MIT-Cre-infected cells underwent a proliferative block and apoptosis and died within 3 days (data not shown). To overcome this and allow for sufficient numbers of viable cells to be harvested, we first transduced the cells with a retrovirus (MSCV–Bcl-x_L) that encodes the antiapoptotic Bcl-x_L factor and cultured these cells for 2 days prior to superinfection with either MIT or MIT-Cre. Proliferation was rescued in the MIT-Cre cultures, and cells were collected 3 days after secondary infection for analysis.

It was essential for quantitative comparisons to determine the percentage of B220$^+$ cells infected under both conditions. Taking advantage of the *Thy-1.1* marker encoded in both vectors, we observed by flow cytometry that control and *Cre*-deleted B220$^+$ B cell progenitors showed comparable transduction efficiencies (>75%) (Fig. 6B). Since MIT-Cre-infected cells required Bcl-x_L expression to bypass apoptosis, it was crucial to check their pro-

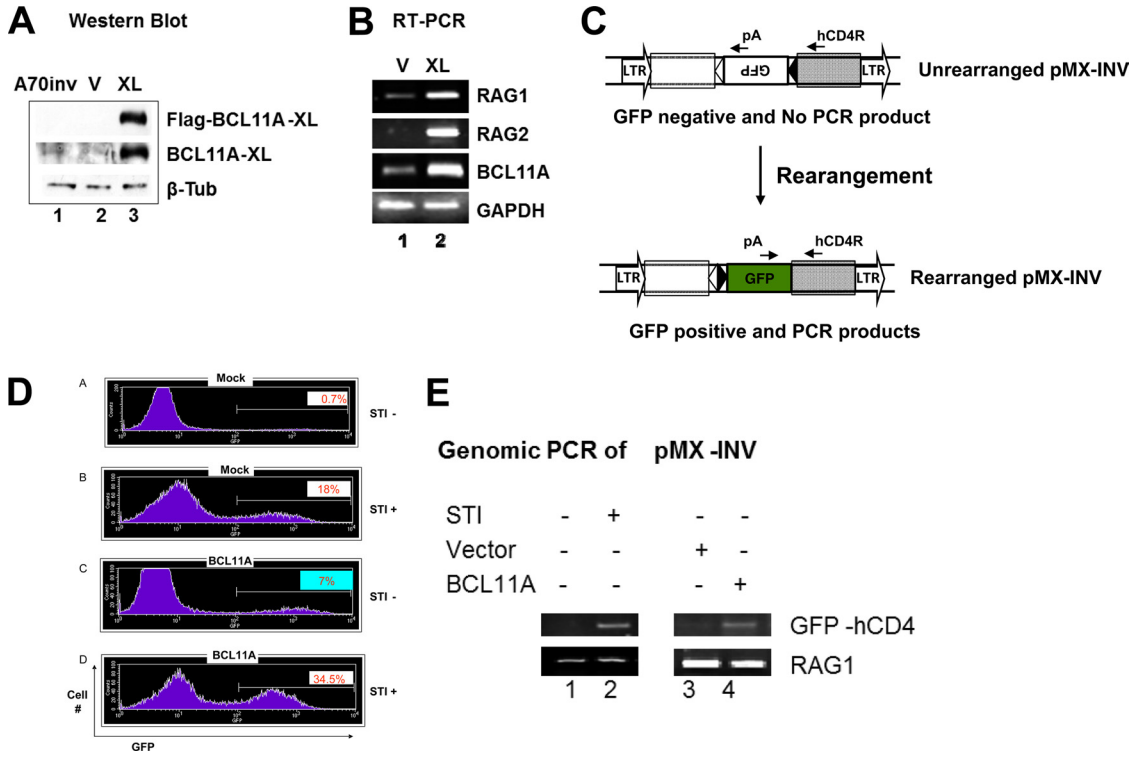

FIG 5 Enforced expression of BCL11A-XL in A70-INV pre-B cells induces V(D)J recombination. (A and B) Establishment of stable overexpression in A70-INV pre-B cells. Transductions and drug selection are described in the legend of Fig. 4A. (A) Anti-Flag Western detection of ectopic BCL11A-XL and anti-BCL11A immunoblotting detection of total expression of BCL11A-XL. β-Tubulin served as a loading control. (B) Transduction of A70-INV cells with BCL11A-XL upregulates RAG1 and RAG2 mRNA relative to mock-transduced cells. GAPDH was the loading control. (C) Schematic diagram of recombination signal sequence (RSS) (black and white triangles)-mediated inversion within the integrated retroviral RAG substrate in A70-INV pre-B cells. Primers used to amplify the inversion are denoted by arrows. (D) Flow cytometry detection of enhanced V(D)J recombination substrate inversion in A70-INV pre-B cells overexpressing BCL11A-XL (XL) or treated with the Abelson kinase inhibitor STI571. Cells were transduced as described in the preceding figure legends and then incubated in the absence (STI−) or in the presence (STI+) of STI571 at 3 μM for 72 h. Inversion of pMX-INV resulted in GFP expression, which was quantified by fluorescence-activated cell sorter analysis following exclusion of dead cells by forward- and side-scatter characteristics. The *x* axis shows GFP intensity; the *y* axis shows cell numbers. Percentages of GFP-positive cells are noted in each plot. (E) PCR validation of RSS-mediated inversion of pMX-INV substrates. Genomic DNA was isolated from the indicated cell lines for PCR according to the strategy and primers described above for panel C. STI571 (STI) treatment (3 μM for 48 h) or transduction with BCL11A-XL retrovirus induced inversion of GFP, allowing PCR amplification (lanes 2 and 4). PCR amplification of the endogenous *Rag1* gene (which is unaffected by RSS-mediated recombination) provided a DNA loading control.

liferative status, particularly since both V(D)J recombination and RAG2 expression are regulated at the G_1 phase of the cell cycle (48). As shown in Fig. 6C, comparable cell cycle progression within normal limits for diploid cells was observed for control and Cre-deleted cultures.

To quantify the extent of Cre-mediated *Bcl11a*$^{L/L}$ deletion and VJκ reduction at the DNA level, we employed 5-fold dilutions of genomic DNA analyzed by both semiquantitative and real-time PCR by using the scheme shown in Fig. 6A. Figure 6D shows the normalized, real-time fold reduction values, indicated under each corresponding ethidium bromide-stained, semiquantitative PCR band for the MIT-Cre condition (calculation is further detailed in the legend). VJκ rearrangement was strongly reduced (average of 15-fold) in direct correlation with *Bcl11a* deletion (~22-fold). This was paralleled by a dramatic reduction (13- to 19-fold) in Rag1, Rag2, and Bcl11a transcript levels (Fig. 6E).

BCL11A-XL overexpression upregulates additional genes implicated in V(D)J recombination and pro-pre-B cell progression. In addition to RAGs, transcription of several genes previously shown to encode proteins involved in V(D)J recombination were modulated following BCL11A-XL overexpression in A70 pre-B cells (Fig. 7). Both interferon-regulatory factor 4 (IRF4) and IRF8 were strongly upregulated by BCL11A-XL overexpression. Upregulation of these transcription factors has been reported to be essential for Ig light chain recombination (49). We also observed consistent upregulation of Foxp1 and FoxO1, factors previously shown to activate RAG via binding to *Erag* (8, 11). Conversely, the *Erag* binding activators E2a and FoxO1 remained unchanged. Igκ germ line transcription, often observed as a consequence of chromatin accessibility of the Jκ locus (7), and the λ5 chain of the pre-B cell receptor were unaffected, whereas its partner subunit, Vpre-B, was strongly upregulated by BCL11A-XL. Inspection of the ENCODE human B cell GM12878 ChIPseq data for BCL11A (28) indicated strong binding peaks within 2 kb up- or downstream of the transcriptional start sites of *VpreB*, *FoxO1*, *IRF8*, and *IRF4*, suggesting that these loci are also directly targeted by BCL11A.

Transcript modulation following STI571 treatment correlated only modestly with that induced by BCL11A-XL overexpression, further emphasizing the different mechanisms of these two RAG activators. For example, and as observed for other Abelson pre-B cell lines (6), STI571 induced expression of Spi-B and Igκ germ

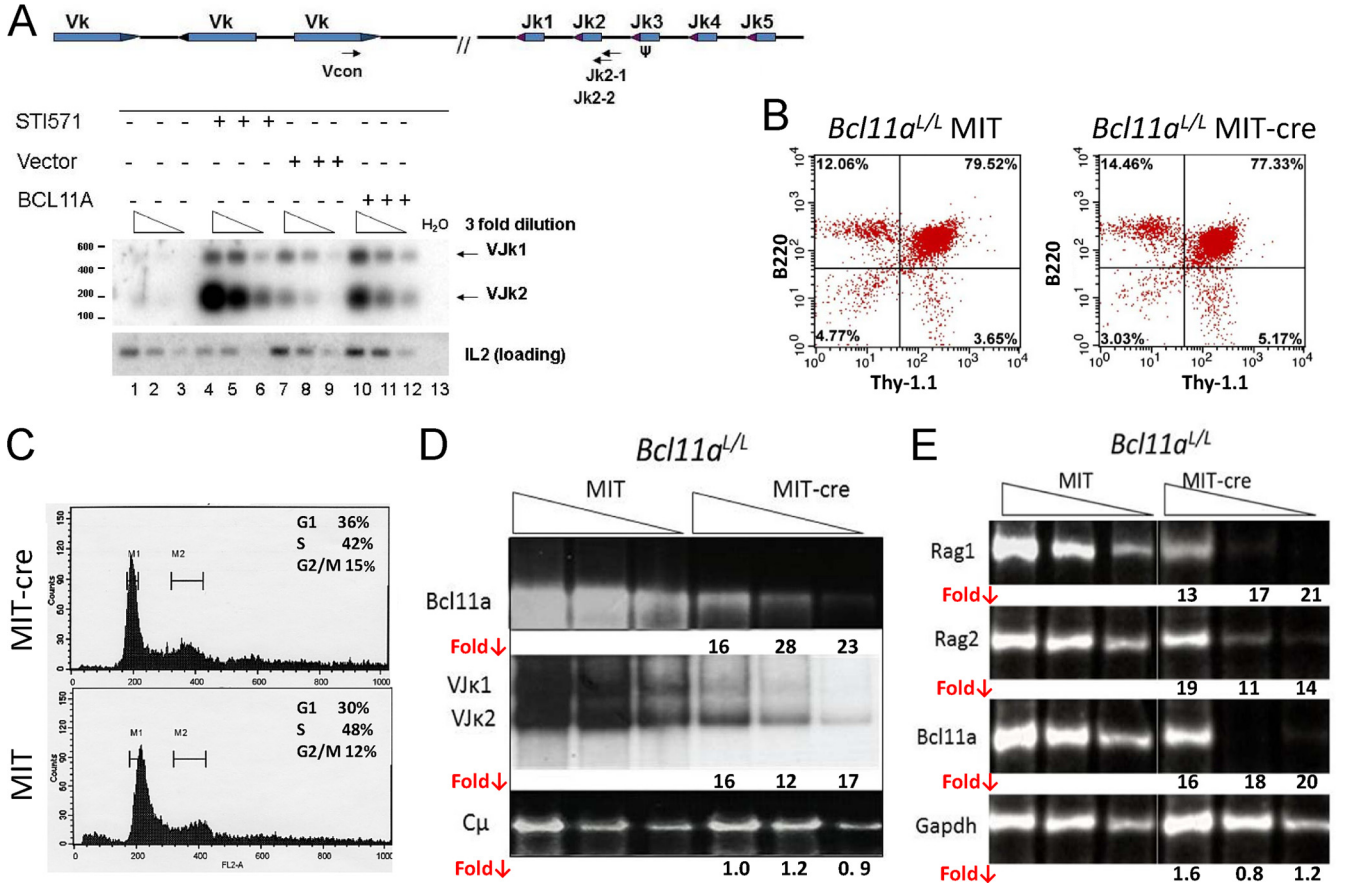

FIG 6 Modulation of BCL11A expression modulates V(D)J rearrangement. (A) BCL11A-XL overexpression induces Vκ-Jκ recombination in A70-INV pre-B cells. A degenerate Vκ consensus primer (Vcon) and a Jκ2-1 reverse primer (top) were used to amplify rearrangements from genomic DNA diluted in 3-fold increments (triangles) to ensure nonsaturating semiquantitative PCR. The strategy predicted products of 190 bp (VJκ2) and 540 bp (VJκ1). Amplified DNA was resolved on agarose gels, transferred onto nylon membranes, and then visualized by autoradiography following hybridization to a Jκ2-2 probe (top). (B) Flow cytometric analysis of *Bcl11a*$^{L/L}$ bone marrow following primary infection with MSCV-Bcl-x$_L$ retrovirus and secondary superinfection with Thy-1.1-expressing MIT or MIT-Cre retroviruses. Cells were stained with antibodies directly conjugated to phycoerythrin (PE-B220) and fluorescein isothiocyanate (FITC–Thy-1.1). (C) Flow cytometric analysis of DNA content/cell cycle progression of *Bcl11a*$^{L/L}$ bone marrow following the retroviral infection protocol detailed above for panel B. Detergent-permeabilized cells were stained with propidium iodide and analyzed as described in Materials and Methods, using CellQuest software to calculate percentages (denoted in right corners) of G_1 (M_1)-, G_2/M (M_2)-, and S (M_1-M_2 interval)-phase cells. (D) Cre recombinase-mediated deletion of *loxP*-modified *Bcl11a* alleles (*Bcl11a*$^{L/L}$) blocks Vκ-Jκ recombination in pre-B cell/IL-7 bone marrow (BM) cultures. Following retroviral infection, detailed as described above for panel B, semiquantitative and real-time PCR of genomic DNA was performed on samples serially diluted 5-fold (triangles). DNA amplified semiquantitatively was gel fractionated and visualized either directly by ethidium bromide staining (top and bottom) or following hybridization (middle), as described above for panel A. PCRs of Cμ served as loading controls. Real-time PCR values, shown as fold reduction (↓) below corresponding lanes, were determined for each DNA dilution by dividing each MIT control value by the corresponding MIT-Cre value. The analyses are representative of 4 independent experiments performed with 4 separate BM isolates. (E) Rag1, Rag2, and Bcl11a transcript levels are significantly reduced following MIT-Cre-mediated deletion of *Bcl11a*$^{L/L}$ in B220$^+$ BM pre-B cell cultures. Total RNA was converted to cDNA and subjected to amplification by semiquantitative RT-PCR or real-time quantitative RT-PCR. cDNA was serially diluted (triangles), fractionated, and analyzed as described above for panel B, with GAPDH dilutions serving as the control.

line transcription (Fig. 7). However, in contrast to data from a previous report (47), we observed robust STI571 repression of IRF4 and IRF8 in A70 cells. Perhaps, the difference lies in the cell lines employed. The previous results (47) were obtained with the Abelson pre-B 200-8 line, which in our hands undergoes massive cell death within 24 h of STI571 treatment (data not shown). The constitutive expression of the *Bcl2* transgene in A70 cells (39) allowed us to analyze events even 4 to 6 days following STI571 treatment without cell death.

DISCUSSION

BCL11A was identified as a proto-oncogene implicated in multiple B cell malignancies (26, 28, 29) and represents one of ~200 "ultraconserved" genes in the human genome (19). Initially thought to be exclusive to B cells, BCL11A is the first genetically and functionally validated transcriptional regulator of both developmental control of globin switching and silencing of γ-globin expression in humans (41, 50). While targeted knockout (25, 32) identified *Bcl11a* as being essential for normal B cell development in the mouse, the transcriptional mechanism and direct targets of its action are incompletely understood.

We initially identified *RAG1* as a potential target gene of the major BCL11A isoform (BCL11A-XL) by microarray analysis (Fig. 2A). Both it and *RAG2* were confirmed by a combination of BCL11A-XL overexpression and shRNA knockdown (Fig. 2B and C). In principle, BCL11A-XL might regulate *RAG* gene expression

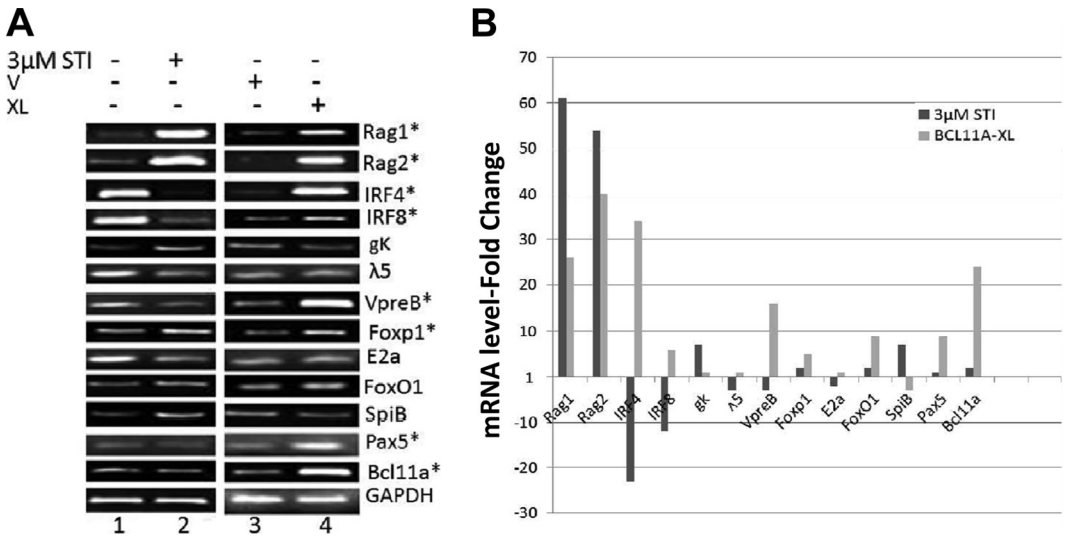

FIG 7 Comparison of BCL11A-XL overexpression with STI571 induction of V(D)J recombination-associated genes. A70-INV pre-B cells were treated with STI571 (3 μM for 20 h) or were stably transduced with BCL11A-XL (XL) or empty virus (V), as described in the legend of Fig. 4. (A) Semiquantitative RT-PCR analysis. cDNA was amplified under linear conditions, gel fractionated, and visualized by ethidium bromide staining of cDNA. GAPDH was the loading control. Asterisks denote transcripts that were consistently upregulated in at least 4 independent experiments. (B) Real-time quantitative RT-PCR analysis. Assays were performed in triplicate and analyzed by the standard curve method (42, 43), by normalization to GAPDH. Fold changes for STI571 values are plotted relative to values for untreated controls, and fold changes for BCL11A-XL values are plotted relative to empty vector (V) controls, with both controls arbitrarily set at a value of 1.

either directly by interacting with *cis*-regulatory elements within the *RAG* locus or indirectly by affecting other pathways that ultimately impact RAG expression. To discriminate between these possibilities, we observed both by BCL11A chromatin occupancy and by *in vitro* DNA binding using pro-B, pre-B, and mature B cell lines that BCL11A was recruited to discrete regions of chromatin within the *RAG1* promoter and the *Erag* enhancer but not within the *RAG2* promoter (Fig. 1A and 3). Transcriptional reporter studies in mouse pre-B cells suggested that two BCL11A binding sites within the *Rag1* promoter synergize to activate transcription (Fig. 4B). The more promoter-distal BCL11A binding site conveyed much stronger (>4-fold) *Erag* enhancement (Fig. 4B). Further consistent with the binding studies, BCL11A-XL failed to drive *Rag2* transcription unless *Erag* was appended to the construct (Fig. 4B). High-resolution, genome-wide ChIPseq, derived publically from the human B cell lymphoma GM12878 (28; http://www.factorbook.org/mediawiki/index.php/BCL11A) and from the human pre-B ALL REH (our unpublished data), identified BCL11A binding sites corresponding to those identified here (Fig. 3F) as well as several others scattered across the *RAG* locus (data not shown). This, along with the finding (29, 35) that within the expansive βγ-globin locus, BCL11A tends to associate with distal control elements rather than proximal promoters, prompts caution as to overly simplified conclusions of the relative importance of any single BCL11A binding site within this complex regulatory locus. The genome-wide ChIP data (28) further indicate that the 500 strongest BCL11A sites within the genome overlap PU.1 sites. Similarly, equivalent genome-wide ENCODE data for PU.1 ChIPseq (28; http://www.factorbook.org/mediawiki/index.php/PU.1) indicated with high statistical significance ($P < 1.0^{-11}$) that a large proportion of PU.1 peaks are in close vicinity to BCL11A peaks. Taken with our EMSA data shown in Fig. 3B, it is highly probable that these factors broadly collaborate or antagonize transcription via closely spaced or even overlapping composite sites.

These findings, along with the observation that recombinant BCL11A-XL failed to bind established target motifs *in vitro*, prompted us to test the transcriptional consequences of enforced BCL11A expression in non-B cells. Unexpectedly, we observed strong repression of *RAG1* promoter-driven transcription in epithelial and fibroblast-derived cell lines, with the more promoter-proximal BCL11A-XL binding site being sufficient to target the activity (Fig. 4B and data not shown). In addition to suggesting that a lineage-restricted cofactor(s) is required for BCL11A-XL to transactivate RAG in lymphoid cells, potential physiologic relevance is provided by the observations that the *RAG1* promoter is not lymphoid restricted (9, 12) and that RAG expression is observed in several nonlymphoid malignant cell types (35, 48, 51–54). Additional relevance may be drawn from the observation that Bcl11a expression within T lineages is limited to double-negative-2 (DN2) stage thymocytes, in which V(D)J recombination of the TcRβ locus initiates (55). At DN3, Bcl11a is extinguished, and expression of its highly similar paralogue, Bcl11b, ensues (56). Although Bcl11b has not previously been implicated in Rag control, $Bcl11b^{-/-}$ thymocytes are impaired in Vβ-Dβ recombination (57).

The domain responsible for both non-B cell repression and pre-B cell activation of BCL11A-XL maps to the N terminus, as deletion of the first 80 amino acids or a single-point mutation (K5/A) within the highly conserved MSRRK motif (Fig. 1B) abrogated both transcriptional activities while retaining normal BCL11A-XL subnuclear localization (Fig. 4B and C and data not shown). The N-terminal motif defines a superfamily of transcription factors crucial to the development, differentiation, and malignancy of several hematopoietic lineages (Fig. 1B) (23, 26, 30, 45, 58). The N terminus, when extended to include the equally conserved C_2HC zinc finger (Fig. 1B), is required for BCL11A-XL to dimerize with itself, with all other BCL11A isoforms (30), and with several corepressor complexes, including NuRD, LSD1/CoREST, NCoR/SMRT, and SIN3 (46, 51; data not shown). Consistent with

this, we observed enhanced BCL11A-XL repression of *RAG1* following coexpression with MTA1, a single member of the 12-membered NuRD complex, which we suspect to be limiting under the conditions which we employed (Fig. 4B and data not shown). Collectively, the results suggest that BCL11A's N-terminal domain is employed in a context-dependent fashion for assembly of both well-characterized corepressor complexes as well as coactivation complexes whose members remain to be defined.

As anticipated, we observed modulation of V(D)J recombination proportional to BCL11A-XL overexpression in cultured A70 pre-B cells (Fig. 5 and 6A) or following Cre-mediated knockdown in cultured explants of $Bcl11a^{L/L}$ bone marrow-derived pre-B cells (Fig. 6B and D). We suggest that the robustness of the effect, particularly in normal pre-B cells that dominate the IL-7 cultures, is derived from both direct transcriptional activation by BCL11A-XL of the *RAG* locus and upregulation of additional transcription factors that either perform the redundant function or act to promote chromatin accessibility of the *V(D)J* locus (Fig. 7). Validated examples of the first group include FOXP1, which transactivates *RAG* directly via binding to *Erag* (Fig. 1A and 3) (8, 11). Elevation and concerted action of this and similar factors that upregulate *RAG* may be sufficient for the *V*κ-*J*κ inversion of the exogenous recombination target *pMX-INV* (Fig. 5C and D). Examples of the second category, which have been shown to be required for chromatin accessibility of the endogenous *V(D)J* locus, include IRF4 and IRF8 (Fig. 7). V(D)J recombination and B cell development are blocked in *IRF4/IRF8* double knockout mice at the pre-B cell stage (49). Accessibility and recombination of Vκ-Jκ has been correlated with selected posttranslational modifications of nucleosomal histone (H) tails (59–61). Ectopic expression of IRF4 in $IRF4/8^{-/-}$ pre-B cells was shown to increase acetylation of H3K9 and H4K14 as well as trimethylation of H3K4, marks associated with active chromatin (49). However, induction of Jκ-Cκ germ line transcription, a second feature typically but not always (62) associated with locus accessibility, was not observed following BCL11A-XL overexpression (Fig. 7). Perhaps, the concomitant lack of BCL11A-XL upregulation of Spi-B (Fig. 7), which, along with IRF4, has been reported to be sufficient for inducing Igκ germ line transcripts (36), is rate limiting under these conditions. Resolution will require a careful assessment of BCL11A-mediated germ line transcription and histone epigenetic alterations across this locus.

Consistent with a recent report by Yu et al. (32), we observed significantly reduced proliferation and increased apoptosis relative to controls in floxed cultures of $Bcl11a^{L/L}$ $B220^{+}$ bone marrow pre-B cells (Fig. 6 and data not shown). In further agreement with that report (32), prior infection of $Bcl11a^{L/L}$ cells with a Bcl-x_L-encoding retrovirus bypassed Cre-mediated apoptosis and proliferation. $Bcl11a^{-/-}$ fetal liver hematopoietic progenitors suffer a severe pre-pro-B cell block (57), typically as a consequence of a proliferative defect in IL-7R signaling (63, 64) or a defect in V(D)J recombination (6). The weight of data assembled here, along with the observations (25, 32, 50, 55) that Bcl11a expression in mouse hematopoiesis initiates at the hematopoietic stem cell stage, suggests that the initial D-J recombination step of antigen receptor assembly will be impaired by conditional *Bcl11a* deficiency. It may be informative that Foxp1, a putative target of BCL11A-XL (Fig. 7), activates this earliest RAG-mediated step of V(D)J joining (11). Further *in vivo* studies in the context of potential collaborating transcription factors such as Foxp1 and PU.1 are required to elucidate whether Bcl11a is, indeed, at the top of the hierarchy of V(D)J transcriptional control.

ACKNOWLEDGMENTS

We thank Chhaya Das, Maya Ghosh, and June Harriss for excellent technical support. We thank Mark Schlissel for sharing luciferase constructs. We thank members of our laboratory for critically reading the manuscript and Paul Das for its preparation.

G.C.I. acknowledges support from NIH grant F32-CA110624, and P.W.T. acknowledges support from NIH grant RO1-CA31534, the Cancer Prevention Research Institute (grant CPRIT RP100612), and the Marie Betzner Morrow Endowment.

REFERENCES

1. **van Gent DC, McBlane JF, Ramsden DA, Sadofsky MJ, Hesse JE, Gellert M.** 1995. Initiation of V(D)J recombination in a cell-free system. Cell **81**:925–934.
2. **Oettinger MA, Schatz DG, Gorka C, Baltimore D.** 1990. RAG-1 and RAG-2, adjacent genes that synergistically activate V(D)J recombination. Science **248**:1517–1523.
3. **Mombaerts P, Iacomini J, Johnson RS, Herrup K, Tonegawa S, Papaioannou VE.** 1992. RAG-1-deficient mice have no mature B and T lymphocytes. Cell **68**:869–877.
4. **Shinkai Y, Rathbun G, Lam KP, Oltz EM, Stewart V, Mendelsohn M, Charron J, Datta M, Young F, Stall AM.** 1992. RAG-2-deficient mice lack mature lymphocytes owing to inability to initiate V(D)J rearrangement. Cell **68**:855–867.
5. **McBlane JF, van Gent DC, Ramsden DA, Romeo C, Cuomo CA, Gellert M, Oettinger MA.** 1995. Cleavage at a V(D)J recombination signal requires only RAG1 and RAG2 proteins and occurs in two steps. Cell **83**:387–395.
6. **Schatz DG.** 2004. V(D)J recombination. Immunol. Rev. **200**:5–11.
7. **Amin RH, Schlissel MS.** 2008. Foxo1 directly regulates the transcription of recombination-activating genes during B cell development. Nat. Immunol. **9**:613–622.
8. **Dengler HS, Baracho GV, Omori SA, Bruckner S, Arden KC, Castrillon DH, DePinho RA, Rickert RC.** 2008. Distinct functions for the transcription factor FoxO1 at various stages of B cell differentiation. Nat. Immunol. **9**:1388–1398.
9. **Fuller K, Storb U.** 1997. Identification and characterization of the murine Rag1 promoter. Mol. Immunol. **34**:939–954.
10. **Hsu LY, Lauring J, Liang HE, Greenbaum S, Cado D, Zhuang Y, Schlissel MS.** 2003. A conserved transcriptional enhancer regulates RAG gene expression in developing B cells. Immunity **19**:105–117.
11. **Hu H, Wang B, Borde M, Nardone J, Maika S, Allred L, Tucker PW, Rao A.** 2006. Foxp1 is an essential transcriptional regulator of B cell development. Nat. Immunol. **7**:819–826.
12. **Kishi H, Jin ZX, Wei XC, Nagata T, Matsuda T, Saito S, Muraguchi A.** 2002. Cooperative binding of c-Myb and Pax-5 activates the RAG-2 promoter in immature B cells. Blood **99**:576–583.
13. **Lauring J, Schlissel MS.** 1999. Distinct factors regulate the murine RAG-2 promoter in B- and T-cell lines. Mol. Cell. Biol. **19**:2601–2612.
14. **Ochiai K, Maienschein-Cline M, Mandal M, Triggs JR, Bertolino E, Sciammas R, Dinner AR, Clark MR, Singh H.** 2012. A self-reinforcing regulatory network triggered by limiting IL-7 activates pre-BCR signaling and differentiation. Nat. Immunol. **13**:300–307.
15. **Verkoczy L, Ait-Azzouzene D, Skog P, Martensson A, Lang J, Duong B, Nemazee D.** 2005. A role for nuclear factor kappa B/rel transcription factors in the regulation of the recombinase activator genes. Immunity **22**:519–531.
16. **Wei XC, Dohkan J, Kishi H, Wu CX, Kondo S, Muraguchi A.** 2005. Characterization of the proximal enhancer element and transcriptional regulatory factors for murine recombination activating gene-2. Eur. J. Immunol. **35**:612–621.
17. **Wei XC, Kishi H, Jin ZX, Zhao WP, Kondo S, Matsuda T, Saito S, Muraguchi A.** 2002. Characterization of chromatin structure and enhancer elements for murine recombination activating gene-2. J. Immunol. **169**:873–881.
18. **Borghesi L, Aites J, Nelson S, Lefterov P, James P, Gerstein R.** 2005. E47 is required for V(D)J recombinase activity in common lymphoid progenitors. J. Exp. Med. **202**:1669–1677.

19. **Reynaud D, Demarco IA, Reddy KL, Schjerven H, Bertolino E, Chen Z, Smale ST, Winandy S, Singh H.** 2008. Regulation of B cell fate commitment and immunoglobulin heavy-chain gene rearrangements by Ikaros. Nat. Immunol. **9**:927–936.
20. **Fell HP, Smith RG, Tucker PW.** 1986. Molecular analysis of the t(2;14) translocation of childhood chronic lymphocytic leukemia. Science **232**: 491–494.
21. **Mitelman F, Johansson B, Mertens F.** 2004. Fusion genes and rearranged genes as a linear function of chromosome aberrations in cancer. Nat. Genet. **36**:331–334.
22. **Richardson AL, Humphries CG, Tucker PW.** 1992. Molecular cloning and characterization of the t(2;14) translocation associated with childhood chronic lymphocytic leukemia. Oncogene **7**:961–970.
23. **Satterwhite E, Sonoki T, Willis TG, Harder L, Nowak R, Arriola EL, Price HP, Gesk S, Steinemann D, Schlegelberger B, Oscier DG, Siebert R, Tucker PW, Dyer MJ.** 2001. The BCL11 gene family: involvement of BCL11A in lymphoid malignancies. Blood **98**:3413–3420.
24. **Avram D, Fields A, Pretty On Top K, Nevrivy DJ, Ishmael JE, Leid M.** 2000. Isolation of a novel family of C(2)H(2) zinc finger proteins implicated in transcriptional repression mediated by chicken ovalbumin upstream promoter transcription factor (COUP-TF) orphan nuclear receptors. J. Biol. Chem. **275**:10315–10322.
25. **Liu P, Keller JR, Ortiz M, Tessarollo L, Rachel RA, Nakamura T, Jenkins NA, Copeland NG.** 2003. Bcl11a is essential for normal lymphoid development. Nat. Immunol. **4**:525–532.
26. **Matthews JM, Kowalski K, Liew CK, Sharpe BK, Fox AH, Crossley M, MacKay JP.** 2000. A class of zinc fingers involved in protein-protein interactions biophysical characterization of CCHC fingers from fog and U-shaped. Eur. J. Biochem. **267**:1030–1038.
27. **Pulford K, Banham AH, Lyne L, Jones M, Ippolito GC, Liu H, Tucker PW, Roncador G, Lucas E, Ashe S, Stockwin L, Walewska R, Karran L, Gascoyne RD, Mason DY, Dyer MJ.** 2006. The BCL11A-XL transcription factor: its distribution in normal and malignant tissues and use as a marker for plasmacytoid dendritic cells. Leukemia **20**:1439–1441.
28. **Raney BJ, Cline MS, Rosenbloom KR, Dreszer TR, Learned K, Barber GP, Meyer LR, Sloan CA, Malladi VS, Roskin KM, Suh BB, Hinrichs AS, Clawson H, Zweig AS, Kirkup V, Fujita PA, Rhead B, Smith KE, Pohl A, Kuhn RM, Karolchik D, Haussler D, Kent WJ.** 2011. ENCODE whole-genome data in the UCSC genome browser (2011 update). Nucleic Acids Res. **39**:D871–D875. doi:10.1093/nar/gkq1017.
29. **Sankaran VG, Xu J, Ragoczy T, Ippolito CG, Walkley CR, Maika SD, Fujiwara Y, Ito M, Groudine M, Bender MA, Tucker PW, Orkin SH.** 2009. Developmental and species-divergent globin switching are driven by BCL11A. Nature **460**:1093–1097.
30. **Liu H, Ippolito GC, Wall JK, Niu T, Probst L, Lee BS, Pulford K, Banham AH, Stockwin L, Shaffer AL, Staudt LM, Das C, Dyer MJ, Tucker PW.** 2006. Functional studies of BCL11A: characterization of the conserved BCL11A-XL splice variant and its interaction with BCL6 in nuclear paraspeckles of germinal center B cells. Mol. Cancer **5**:18. doi:10.1186/1476-4598-5-18.
31. **Suzuki T, Shen H, Akagi K, Morse HC, Malley JD, Naiman DQ, Jenkins NA, Copeland NG.** 2002. New genes involved in cancer identified by retroviral tagging. Nat. Genet. **32**:166–174.
32. **Yu Y, Wang J, Khaled W, Burke S, Li P, Chen X, Yang W, Jenkins NA, Copeland NG, Zhang S, Liu P.** 2012. Bcl11a is essential for lymphoid development and negatively regulates p53. J. Exp. Med. **209**:2467–2483.
33. **Sandelin A, Bailey P, Bruce S, Engstrom PG, Klos JM, Wasserman WW, Ericson J, Lenhard B.** 2004. Arrays of ultraconserved non-coding regions span the loci of key developmental genes in vertebrate genomes. BMC Genomics **5**:99. doi:10.1186/1471-2164-5-99.
34. **Xu J, Cong P, Sankaran VG, Shao Z, Esrick EB, Chong BG, Ippolito GC, Fujiwara Y, Ebert BL, Tucker PW, Orkin SH.** 2011. Correction of sickle cell disease in adult mice by interference with fetal hemoglobin silencing. Science **334**:993–996.
35. **Xu J, Sankaran VG, Ni M, Menne TF, Puram RV, Kim W, Orkin SH.** 2010. Transcriptional silencing of gamma-globin by BCL11A involves long-range interactions and cooperation with SOX6. Genes Dev. **24**:783–798.
36. **Ma S, Pathak S, Trinh L, Lu R.** 2008. Interferon regulatory factors 4 and 8 induce the expression of Ikaros and Aiolos to downregulate pre-B-cell receptor and promote cell-cycle withdrawal in pre-B-cell development. Blood **111**:1396–1403.
37. **Shaffer AL, Yu X, He Y, Boldrick J, Chan EP, Staudt LM.** 2000. BCL-6 represses genes that function in lymphocyte differentiation, inflammation, and cell cycle control. Immunity **13**:199–212.
38. **Ngo V, Davis R, Lamy L, Yu X, Zhao H, Lenz G, Lam L, Dave S, Yang L, Powell J.** 2006. A loss-of-function RNA interference screen for molecular targets in cancer. Nature **441**:106–110.
39. **Bredemeyer AL, Sharma GG, Huang CY, Helmink BA, Walker LM, Khor KC, Nuskey B, Sullivan KE, Pandita TK, Bassing CH, Sleckman BP.** 2006. ATM stabilizes DNA double-strand-break complexes during V(D)J recombination. Nature **442**:466–470.
40. **Nakamura T, Yamazaki Y, Saiki Y, Moriyama M, Largaespada DA, Jenkins NA, Copeland NG.** 2000. Evi9 encodes a novel zinc finger protein that physically interacts with BCL6, a known human B-cell proto-oncogene product. Mol. Cell. Biol. **20**:3178–3186.
41. **Ramsden D.** 1994. Kappa light chain rearrangement in mouse fetal liver. J. Immunol. **153**:1150–1160.
42. **Fu WJ, Hu J, Spencer T, Carroll R, Wu G.** 2006. Statistical models in assessing fold change of gene expression in real-time RT-PCR experiments. Comput. Biol. Chem. **30**:21–26.
43. **Yuan JS, Reed A, Chen F, Stewart CN.** 2006. Statistical analysis of real-time PCR data. BMC Bioinformatics **7**:85. doi:10.1186/1471-2105-7-85.
44. **Reyes JC, Muchardt C, Yaniv M.** 1997. Components of the human SWI/SNF complex are enriched in active chromatin and are associated with the nuclear matrix. J. Cell Biol. **137**:263–274.
45. **Tsang AP, Visvader JE, Turner CA, Fujiwara Y, Yu C, Weiss MJ, Crossley M, Orkin SH.** 1997. FOG, a multitype zinc finger protein, acts as a cofactor for transcription factor GATA-1 in erythroid and megakaryocytic differentiation. Cell **90**:109–119.
46. **Cismasiu VB, Adamo K, Gecewicz J, Duque J, Lin Q, Avram D.** 2005. BCL11B functionally associates with the NuRD complex in T lymphocytes to repress targeted promoter. Oncogene **24**:6753–6764.
47. **Muljo S, Schlissel M.** 2003. A small molecule Abl kinase inhibitor induces differentiation of Abelson virus-transformed pre-B cell lines. Nat. Immunol. **4**:31–37.
48. **Lin WC, Desiderio S.** 1994. Cell cycle regulation of V(D)J recombination-activating protein RAG-2. Proc. Natl. Acad. Sci. U. S. A. **91**:2733–2737.
49. **Lu R, Medina KL, Lancki DW, Singh H.** 2003. IRF-4,8 orchestrate the pre-B-to-B transition in lymphocyte development. Genes Dev. **17**:1703–1708.
50. **Su AI, Wiltshire T, Batalov S, Lapp H, Ching KA, Block D, Zhang J, Soden R, Hayakawa M, Kreiman G, Cooke MP, Walker JR, Hogenesch JB.** 2004. A gene atlas of the mouse and human protein-encoding transcriptomes. Proc. Natl. Acad. Sci. U. S. A. **101**:6062–6067.
51. **Chen Z, Xiao Y, Zhang J, Li J, Liu Y, Zhao Y, Ma C, Luo J, Qiu Y, Huang G, Korteweg C, Gu J.** 2011. Transcription factors E2A, FOXO1 and FOXP1 regulate recombination activating gene expression in cancer cells. PLoS One **6**:e20475. doi:10.1371/journal.pone.0020475.
52. **Laszkiewicz A, Sniezewski L, Kasztura M, Bzdzion L, Cebrat M, Kisielow P.** 2012. Bidirectional activity of the NWC promoter is responsible for RAG-2 transcription in non-lymphoid cells. PLoS One **7**:e44807. doi:10.1371/journal.pone.0044807.
53. **Qiu X, Zhu X, Zhang L, Mao Y, Zhang J.** 2003. Human epithelial cancers secrete immunoglobulin G with unidentified specificity to promote growth and survival of tumor cells. Cancer Res. **63**:6488–6495.
54. **Zheng H, Li M, Liu H, Ren W, Hu DS, Shi Y, Tang M, Cao Y.** 2007. Immunoglobulin alpha heavy chain derived from human epithelial cancer cells promotes the access of S phase and growth of cancer cells. Cell Biol. Int. **31**:82–87.
55. **Seita J, Sahoo D, Rossi DJ, Bhattacharya D, Serwold T, Inlay MA, Ehrlich LI, Fathman JW, Dill DL, Weissman IL.** 2012. Gene Expression Commons: an open platform for absolute gene expression profiling. PLoS One **7**:e40321. doi:10.1371/journal.pone.0040321.
56. **Wakabayashi Y, Watanabe H, Inoue J, Takeda N, Sakata J, Mishima Y, Hitomi J, Yamamoto T, Utsuyama M, Niwa O, Aizawa S, Kominami R.** 2003. Bcl11b is required for differentiation and survival of αβ T lymphocytes. Nat. Immunol. **4**:533–539.
57. **Inoue J, Kanefuji T, Okazuka K, Watanabe H, Mishima Y, Kominami R.** 2006. Expression of TCR alpha beta partly rescues developmental arrest and apoptosis of alpha beta T cells in Bcl11b−/− mice. J. Immunol. **176**: 5871–5879.
58. **Bond HM, Mesuraca M, Caarbone E, Bonelli P, Agosti V, Amodio N, De Rosa G, Di Nicola M, Gianni AM, Moore MA, Hata A, Grieco M, Morrone G, Venuta S.** 2004. Early hematopoietic zinc finger protein

(EHZF), the human homolog to mouse Evi3, is highly expressed in primitive human hematopoietic cells. Blood **103**:2062–2070.
59. **Fitzsimmons SP, Bernstein RM, Max EE, Skok JA, Shapiro MA.** 2007. Dynamic changes in accessibility, nuclear positioning, recombination, and transcription at the Ig kappa locus. J. Immunol. **179**:5264–5273.
60. **Goldmit M, Ji Y, Skok J, Roldan E, Jung S, Cedar H, Bergman Y.** 2005. Epigenetic ontogeny of the Igk locus during B cell development. Nat. Immunol. **6**:198–203.
61. **Perkins EJ, Kee BL, Ramsden DA.** 2004. Histone 3 lysine 4 methylation during the pre-B to immature B-cell transition. Nucleic Acids Res. **32**: 1942–1947.
62. **Angelin-Duclos C, Calame K.** 1998. Evidence that immunoglobulin VH-DJ recombination does not require germ line transcription of the recombining variable gene segment. Mol. Cell. Biol. **18**:6253–6264.
63. **Corcoran AE, Riddell A, Krooshoop D, Venkitaraman AR.** 1998. Impaired immunoglobulin gene rearrangement in mice lacking the IL-7 receptor. Nature **391**:904–907.
64. **Corcoran AE, Smart FM, Cowling RJ, Crompton T, Owen MJ, Venkitaraman AR.** 1996. The interleukin-7 receptor alpha chain transmits distinct signals for proliferation and differentiation during B lymphopoiesis. EMBO J. **15**:1924–1932.
65. **Brown ST, Miranda GA, Galic Z, Hartman IZ, Lyon CJ, Aguilera RJ.** 1997. Regulation of the RAG-1 promoter by the NF-Y transcription factor. J. Immunol. **158**:5071–5074.